INFN/AE–97/19÷28
19 Giugno 1997

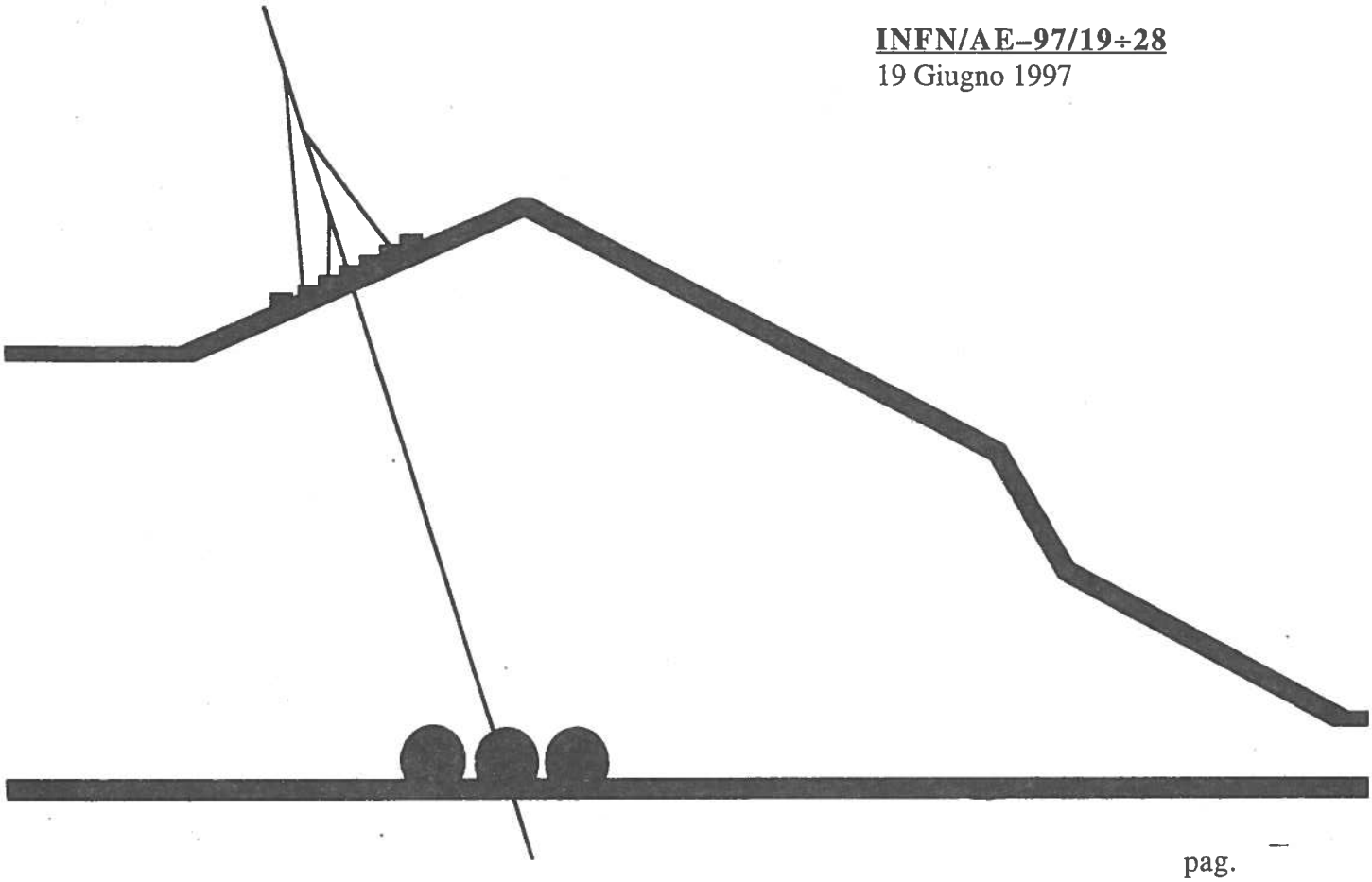

Contributions of the MACRO Collaboration to the 1997 Summer Conferences

INFN – Laboratori Nazionali del Gran Sasso

Published by ***SIS–Pubblicazioni*** *dei Laboratori Nazionali di Frascati*

The MACRO Collaboration

M. Ambrosio[12], R. Antolini[7], G. Auriemma[14,a], R. Baker[11], A. Baldini[13], G. C. Barbarino[12], B. C. Barish[4], G. Battistoni[6,b], R. Bellotti[1], C. Bemporad[13], P. Bernardini[10], H. Bilokon[6], V. Bisi[16], C. Bloise[6], C. Bower[8], S. Bussino[14], F. Cafagna[1], M. Calicchio[1], D. Campana[12], M. Carboni[6], M. Castellano[1], S. Cecchini[2,c], F. Cei[13,d], P. Celio[14], V. Chiarella[6], A. Corona[14], S. Coutu[11], G. De Cataldo[1], H. Dekhissi[2,e], C. De Marzo[1], I. De Mitri[9], M. De Vincenzi[14,f], A. Di Credico[7], O. Erriquez[1], C. Favuzzi[1], C. Forti[6], P. Fusco[1], G. Giacomelli[2], G. Giannini[13,g], N. Giglietto[1], M. Goretti[4,14], M. Grassi[13], L. Gray[7], A. Grillo[7], F. Guarino[12], P. Guarnaccia[1], C. Gustavino[7], A. Habig[3], K. Hanson[11], A. Hawthorne[8], R. Heinz[8], E. Iarocci[6,h], E. Katsavounidis[4], E. Kearns[3], S. Kyriazopoulou[4], E. Lamanna[14], C. Lane[5], D. S. Levin[11], P. Lipari[14], N. P. Longley[4,m], M. J. Longo[11], F. Maaroufi[2,e], G. Mancarella[10], G. Mandrioli[2], S. Manzoor[2,n], A. Margiotta Neri[2], A. Marini[6], D. Martello[10], A. Marzari-Chiesa[16], M. N. Mazziotta[1], C. Mazzotta[10], D. G. Michael[4], S. Mikheyev[7,i], L. Miller[8], P. Monacelli[9], T. Montaruli[1], M. Monteno[16], S. Mufson[8], J. Musser[8], D. Nicoló[13,d], R. Nolty[4], C. Okada[3], C. Orth[3], G. Osteria[12], O. Palamara[10], S. Parlati[7], V. Patera[6,h], L. Patrizii[2], R. Pazzi[13], C. W. Peck[4], S. Petrera[9,10], P. Pistilli[14,f], V. Popa[2,l], V. Pugliese[14], A. Rainó[1], J. Reynoldson[7], F. Ronga[6], U. Rubizzo[12], A. Sanzgiri[15], C. Satriano[14,a], L. Satta[6,h], E. Scapparone[7], K. Scholberg[3,4], A. Sciubba[6,h], P. Serra-Lugaresi[2], M. Severi[14], M. Sioli[2], M. Sitta[16], P. Spinelli[1], M. Spinetti[6], M. Spurio[2], R. Steinberg[5], J. L. Stone[3], L. R. Sulak[3], A. Surdo[10], G. Tarlé[11], V. Togo[2], C. W. Walter[4] and R. Webb[15]

1. Dipartimento di Fisica dell'Università di Bari and INFN, 70126 Bari, Italy
2. Dipartimento di Fisica dell'Università di Bologna and INFN, 40126 Bologna, Italy
3. Physics Department, Boston University, Boston, MA 02215, USA
4. California Institute of Technology, Pasadena, CA 91125, USA
5. Department of Physics, Drexel University, Philadelphia, PA 19104, USA
6. Laboratori Nazionali di Frascati dell'INFN, 00044 Frascati (Roma), Italy

7. Laboratori Nazionali del Gran Sasso dell'INFN, 67010 Assergi (L'Aquila), Italy
8. Depts. of Physics and of Astronomy, Indiana University, Bloomington, IN 47405, USA
9. Dipartimento di Fisica dell'Università dell'Aquila and INFN, 67100 L'Aquila, Italy
10. Dipartimento di Fisica dell'Università di Lecce and INFN, 73100 Lecce, Italy
11. Department of Physics, University of Michigan, Ann Arbor, MI 48109, USA
12. Dipartimento di Fisica dell'Università di Napoli and INFN, 80125 Napoli, Italy
13. Dipartimento di Fisica dell'Università di Pisa and INFN, 56010 Pisa, Italy
14. Dipartimento di Fisica dell'Università di Roma "La Sapienza" and INFN, 00185 Roma, Italy
15. Physics Department, Texas A&M University, College Station, TX 77843, USA
16. Dipartimento di Fisica Sperimentale dell'Università di Torino and INFN, 10125 Torino, Italy
a Also Università della Basilicata, 85100 Potenza, Italy
b Also INFN Milano, 20133 Milano, Italy
c Also Istituto TESRE/CNR, 40129 Bologna, Italy
d Also Scuola Normale Superiore di Pisa, 56010 Pisa, Italy
e Also Faculty of Sciences, University Mohamed I, B.P. 424 Oujda, Morocco
f Also Dipartimento di Fisica, Università di Roma Tre, Roma, Italy
g Also Università di Trieste and INFN, 34100 Trieste, Italy
h Also Dipartimento di Energetica, Università di Roma, 00185 Roma, Italy
i Also Institute for Nuclear Research, Russian Academy of Science, 117312 Moscow, Russia
l Also Institute for Space Sciences, 76900 Bucharest, Romania
m Swarthmore College, Swarthmore, PA 19081, USA
n RPD, PINSTECH, P.O. Nilore, Islamabad, Pakistan

Acknowledgements.

We gratefully acknowledge the support of the director and of the staff of the Laboratori Nazionali del Gran Sasso and the invaluable assistance of the technical staff of the Institutions participating in the experiment. We thank the Istituto Nazionale di Fisica Nucleare (INFN), the U.S. Department of Energy and the U.S. National Science Foundation for their generous support of the MACRO experiment. We thank INFN, ICTP (Trieste) and NATO for providing fellowships and grants (FAI) for non Italian citizens.

MAGNETIC MONOPOLE SEARCH WITH THE MACRO DETECTOR AT GRAN SASSO

INFN/AE–97/19
19 Giugno 1997

ABSTRACT

We present the results of the search for massive magnetic monopoles in the penetrating cosmic radiation performed with the MACRO detector. Independent analyses were carried out by using the scintillator, streamer tubes and track-etch subdetectors in different ranges of the monopole velocities. Since no candidates were found in several years of data taking, present flux upper limits are below the Parker bound for monopole velocities $\geq 10^{-4}c$.

INTRODUCTION

Grand Unified Theories (GUTs) of the electroweak and strong interactions predict the existence of massive ($\sim 10^{17}$ GeV) magnetic monopoles (Preskill, 1979).The MACRO detector at Gran Sasso was conceived to be effective in the search for such monopoles at a sensitivity level well below the Parker bound (10^{-15}cm^{-2} s^{-1} sr^{-1}) (Turner et al., 1982), for a large range of velocities, $4 \times 10^{-5} < \beta < 1$.

MACRO consists of six supermodules with total dimension $77 \times 12 \times 9$ m^3. Each supermodule is divided into a lower and an upper part. The lower part consists of two separate modules made of ten horizontal streamer tube planes (6×12 m^2) interleaved with seven rock absorber layers and two scintillation counter planes (on the top and bottom). The east and west sides (12×5 m^2) of each lower supermodule are closed by a sandwich of two sets of vertical streamer tube planes (three layers each), interleaved with a scintillation counter plane. Two other "vertical detector systems" close the north and south walls. The upper part of each supermodule consists of two vertical detector systems and of a roof made of two sets of two horizontal streamer tube planes interleaved with a scintillation counter plane, without any absorber. The nuclear track subdetector is located horizontally in the middle of the lower MACRO structure, and vertically on the east wall and on the lower part of the north wall.

Special care was taken to ensure that the three types of detectors and the readout electronics were sensitive to low β particles. A single candidate event may provide distinctive and multiple signatures in the three subdetectors, so the experiment has enough redundancy of information to attain unequivocal and reliable interpretation on the basis of only few or even one event. A more detailed description of the apparatus with particular emphasis on monopole detection has been given in (Ahlen et al., 1993, Ambrosio et al., 1997 and Ahlen et al., 1995).

Single subdetector searches with scintillator or streamer tubes are very effective in the low β region, where the background is due to uncorrelated noise and the required rejection power is not too high. Searches for fast magnetic monopoles are heavily affected by the background due to energetic muons with large energy losses in the detector. Although single subdetector searches for fast monopoles have been effectively performed on limited data samples, a combined use of the three redundant systems can achieve the needed rejection by imposing looser requirements.

Present analyses refer only to direct detection of bare monopoles with unit magnetic Dirac charge. Magnetic monopole induced nucleon decay is not considered; the results are then valid for catalysis cross sections smaller than 10 mb. An isotropic flux of magnetic monopoles was also assumed. This applies to monopoles with enough kinetic energy to traverse the Earth. This condition sets a β dependent mass threshold which is $\sim 10^{17}$ GeV for $\beta \sim 5 \cdot 10^{-5}$ and is lower (down to $\sim 10^{10}$ GeV) for faster poles.

SINGLE SUBDETECTOR SEARCHES

Searches Using the Liquid Scintillator

The use of three different triggers, electronics and analysis procedures allows us to cover the entire β range with maximum efficiency.

1. The light yield of magnetic monopoles with $10^{-4} < \beta < 5 \cdot 10^{-3}$ is inferred by the measurement of the light yield of protons with similar velocities in plastic scintillators (Ahlen et al., 1994). The waveform of the photomultiplier output is analysed looking for the long and flat light pulse expected from a monopole. Two independent searches have been performed and published (Ahlenet al., 1994 and Ambrosio et al., 1997). The established flux upper limits for $1.8 \times 10^{-4} < \beta < 3 \times 10^{-3}$ of 5.6 and 4.1×10^{-15} cm^{-2} s^{-1} sr^{-1} are reported in Fig. 1 in curves A and D.

2. In the medium velocity interval the light produced per unit pathlength and the time of flight across the apparatus are used at the same time. In this way the background, mainly due to natural radioactivity and atmospheric muons stopping in the detector, is completely rejected. The analysed data were collected between October 1989 and January 1997. ¿From the absence of monopole candidates the 90% C.L. flux upper limit of 6.0×10^{-16} cm^{-2} s^{-1} sr^{-1} for $1.2 \cdot 10^{-3} < \beta < 10^{-1}$ is reported in Fig. 1 curve B.

3. The huge energy loss of a fast magnetic monopoles ($\beta > 10^{-1}$) tags candidates by searching for events with large amounts of light recorded by photomultipliers. High energy showering muons are the main background for this kind of analysis. Such events are completely removed by checking that the measured energy loss in two scintillator layers is lower than expected for monopoles. The resulting flux upper limit (4.4×10^{-15} cm^{-2} s^{-1} sr^{-1} for $\beta > 10^{-1}$) is reported in curve C of Fig. 1.

In the present analyses the upper part (including the top horizontal layer and the side top vertical layers) was not used. Trigger and analysis efficiencies were checked by pulsing the counters with LED and nitrogen laser light. The 90% flux upper limits are reported in Fig. 1.

Search Using the Streamer Tube Subdetector

The tubes are filled with a 73% He and 27% n-pentane gas mixture and are operated in the limited streamer mode. The presence of the helium allows detection with 100 % efficiency of the passage of a magnetic monopole exploiting the Drell and Penning effects (Ahlen et al., 1995 and Drell et al., 1983). The analysis is based on the search for single tracks and on the measurement of the velocity of the candidates, a complete description of the employed hardware and analysis procedures has been given (Ahlen et al., 1995). Only the horizontal streamer planes of the lower MACRO have been used in the trigger; the upper part and the vertical planes have been used for event reconstruction. The analyzed data sample was collected from February 1992 to April 1997 for a live-time of 1823 days. Since the construction of the apparatus was not yet completed, during the first year of this period the acceptance was only a fraction of the total 4250 m^2 sr of the full lower part of the detector. The trigger and analysis were checked to be velocity independent. The global efficiency was then estimated by computing the ratio of the rate of single muons reconstructed by this analysis to the expected one. The typical overall efficiency was over 90%. A Monte Carlo simulation including all the geometrical and trigger requirements was used to compute the detector acceptance. No candidate remained. For $1.1 \times 10^{-4} < \beta < 5 \times 10^{-3}$ a flux limit $\Phi_M < 5.0 \times 10^{-16}$ cm^{-2} s^{-1} sr^{-1} at 90 % C. L. was obtained.

Search Using the Nuclear Track Subdetector

The nuclear track-etch subdetector (CR39 and LEXAN sheets) covers a surface of 1263 m^2 and the total acceptance for fast magnetic monopoles is about 7100 m^{2}sr. The subdetector is used as a stand

alone detector and in a "triggered mode" by the scintillator and streamer tube systems. The CR39 nuclear track detector was calibrated with slow and fast ions, checking that the response depends on the restricted energy loss only (Ambrosio et al., 1997a). In the last years about 24 m^2/year of track-etch detector were extracted. The method of searching for monopoles and the determination of the geometrical and detection efficiencies are reported in detail in (Ambrosio et al., 1997a). A total surface area of 88.86 m^2 of CR39 has been analysed, with an average exposure time of 5.89 years. No candidate was found; the 90% C.L. upper limits on the magnetic monopole flux are at the level of 2.7×10^{-15} $cm^{-2}s^{-1}sr^{-1}$ at $\beta \sim 1$, and 4.2×10^{-15} $cm^{-2}s^{-1}sr^{-1}$ at $\beta \sim 10^{-4}$, (see Fig. 1, curves "CR39").

COMBINED SEARCHES

As stated before, a combined search for fast magnetic monopoles was also performed. For such velocities the three subdetector responses directly result from the Bethe-Bloch formula applied to a moving magnetic charge. As a consequence a combined search (i.e. a three-fold detector coincidence) can be exploited to reduce the large cosmic ray background.

The analysis procedure uses, at the same time, the data coming from scintillator and streamer subdetectors, while scanning of the track-etch is used as a final tool for rejection/confirmation of the selected candidates. The events are triggered by requiring at least one fired scintillator counter and 7 hit horizontal streamer planes. The fast monopole signature is its large ionizing power with respect to minimum ionizing particles. The event selection criteria are therefore based on the amount of light recorded by the photomultipliers and by both digital (tracking) and analog (pulse charge) information coming from the streamer tubes. Since monopoles with $\beta < 0.99$ lose their energy by means of continuous excitation/ionization processes of the traversed medium, a non-showering single particle is searched for in the tracking system. A pathlength of at least 10 cm in the scintillator volume is imposed in order to guarantee a good measurement of the produced light. The signal detected in each crossed counter is then required to exceed the minimum amount of light produced by a $\beta = 5 \cdot 10^{-3}$ monopole (Ahlen and Tarlé, 1983) with the shortest pathlength accepted in the analysis. Taking into account the 5% resolution and the 10% non-linearity of the detector response at that light level (Ambrosio et al., 1997), a three standard deviation cut is imposed.

A further selection is then applied by using the logarithmic dependence of the streamer tube pulse charge on the particle ionizing power (Battistoni et al., 1988 and Battistoni et al., 1996). Fluctuations resulting from gas mixture and pressure variations are taken into account by calibrating the streamer response with cosmic muons on a run by run basis. After correction for geometrical and electronic non-linear effects (Battistoni et al., 1997), a cut is applied on the mean streamer charge measured along the particle trajectory. As a result of a detailed Monte Carlo simulation of the streamer response, 90% of monopoles with $\beta > 5 \cdot 10^{-3}$ are ensured to pass this analysis step. The few ($\sim$ 5/year) selected candidates are analysed in the appropriate CR39-LEXAN sheets by looking for large restricted energy loss producing a detectable track in this subdetector.

The analysed data refers to 667 live days with an average global efficiency of 74%. The acceptance, computed by means of a full Monte Carlo including all the analysis requirements, is 3565 m^2sr. No candidates survived, the 90% C.L. monopole flux upper limit is $1.5 \cdot 10^{-15} cm^{-2}sr^{-1}s^{-1}$ for $5 \cdot 10^{-3} < \beta < 0.99$.

DISCUSSION AND CONCLUSIONS

No candidates were found in any of the aforementioned searches. The corresponding 90% C.L. flux limits are shown in Fig. 1 as function of β.

As any one of the subdetectors may rule out, within its own acceptance and sensitivity, a potential candidate from the others, the present global MACRO limit may be taken as a combination of separate limits. When two or more analyses were coincident in time, in space and in β, we considered only the one with the larger acceptance in that β range. In the more general case the β-interval was divided into subintervals sufficient to characterize the changes in individual acceptances. In each β-subinterval the

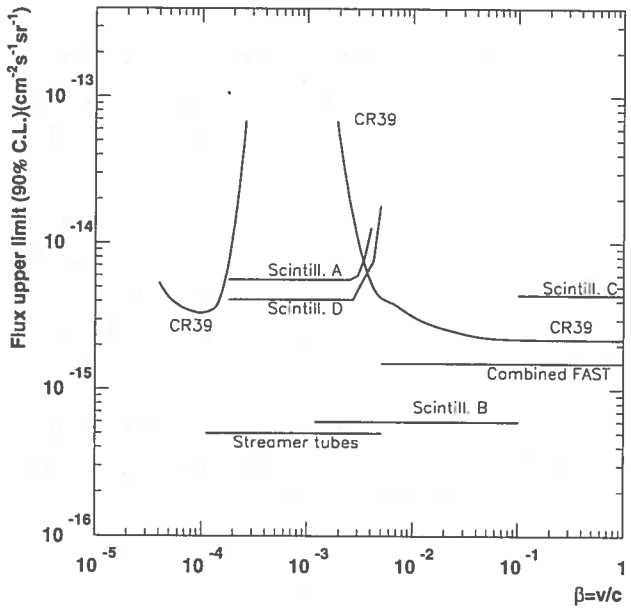

Fig. 1 The 90% C.L. upper limits obtained using the various MACRO subdetectors

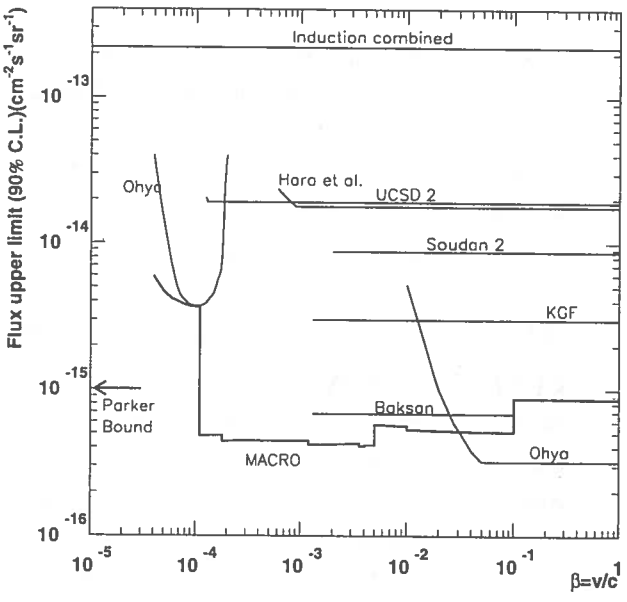

Fig. 2 The 90% C.L. obtained by MACRO (global limit) and by other experiments

MACRO time integrated acceptance was computed as the sum of the independent portions.

The total MACRO limit is computed as $2.3/E_{total}$ where $E_{total} = \sum_i E'_i$, and the E'_i are the independent time integrated acceptances.

This limit is compared in Fig. 2 with the results obtained by other experiments which searched for bare magnetic monopoles with $g = g_D$ and $\sigma_{cat} < 10$ mb (Bermon, 1990, Buckland, 1990, Thron, 1992, Alexeyev, 1990, Orito, 1991, Adarkar, 1990, Hara, 1990).

REFERENCES

Adarkar H. et al. (Kolar gold field monopole experiment), 21^{st} ICRC, Adelaide (1990) 95.

Alexeyev E. N. et al., (A search for superheavy magnetic monopoles by the Baksan underground scintillation telescope), 21^{st} ICRC, Adelaide, vol. 10 (1990) 83.

Ahlen S. P. and Tarlé G., Phys. Rev. D27, 688 (1983)

Ahlen S. P. et al., MACRO Collaboration, Nucl. Instr. & Meth. A 324 (1993) 337.

Ahlen S. P. et al., MACRO Collaboration, Phys. Rev. Lett. 72 (1994) 608.

Ahlen S. P. et al.,MACRO Collaboration, (Search for magnetic monopoles with the MACRO track-etch detector), LNGS-94/115 (1994).

Ahlen S. P. et al., MACRO Collaboration, Astrop. Phys. 4 (1995) 33.

Ambrosio M. et al., MACRO Collaboration, Astrop. Phys. 6 (1997) 113.

Ambrosio M. et al., MACRO Collaboration, Submitted to Phys. Lett. B.

Battistoni G. et al., Nucl. Instr. & Meth. A270 (1988) 185.

Battistoni G. et al., INFN/AE-96/33, submitted to Nucl. Instr. & Meth.

Battistoni G. et al., INFN/AE-97/13, submitted to Nucl. Instr. & Meth.

Bermon S. et al., Phys. Rev. Lett. 64 (1990) 839.

Buckland K. N. et al., Phys. Rev. D 41 (1990) 2726.

Drell S. et al., Phys. Rev. Lett. 50 (1983) 644.

Hara T. et al. (A search experiment for slow moving monopoles ($\beta \geq 2 \times 10^{-4}$) using a helium proportional counters array), 21^{st} ICRC, Adelaide (1990) 79.

Orito S. et al., Phys. Rev. Lett. 66 (1991) 1951.

Preskill J., Phys. Rev. Lett. 43 (1979) 1365.

Thron J. L. et al., Phys. Rev. D 46 (1992) 4846. Turner M. S., Parker E. M. and Bogdan T. J., Phys. Rev. D 26 (1982) 1926; Adams F. C. et al., Phys. Rev. Lett. 70 (1993) 2511.

SEARCH FOR NUCLEARITES WITH THE MACRO DETECTOR AT GRAN SASSO

INFN/AE–97/20
19 Giugno 1997

ABSTRACT

In this paper we present the results of the searches for nuggets of strange quark matter ("nuclearites", "strangelets") using the various subdetectors of the MACRO detector at the Gran Sasso underground laboratory. The upper flux limits refer to data collected from 1989 till August 1 1995, while the experiment was under construction, and from August 2 1995 till April 1997 with the full detector.

INTRODUCTION

Nuggets of strange quark matter (aggregates of u, d and s quarks in equal proportions and electrons that ensure the electrical neutrality) that should be stable for all baryon numbers in the range between ordinary nuclei and neutron stars ($A \sim 10^{57}$) have been hypothesized (Witten, 1984). They could be the ground state of QCD and could have been produced in the primordial Universe or in violent astrophysical processes. Nuclearites could be an important candidate for dark matter.

The main energy loss mechanism for nuclearites passing trough matter is that of atomic collisions. While traversing the medium the nuclearites should displace the matter in their path by elastic or quasi-elastic collisions with the ambient atoms (De Rújula et al., 1984). For typical galactic velocities, nuclearites with masses larger than 0.1 g could traverse the Earth (De Rújula et al., 1984).

Nuclearites could contribute to the missing mass of the Universe. A limit on their local mass density may be estimated assuming that $\Phi_{max.} = \rho_{DM} v/(2\pi M)$, where $\rho_{DM} \simeq 10^{-24}$ g cm^{-3} represents the local dark matter density (De Rújula et al., 1984).

MACRO (Monopole, Astrophysics and Cosmic Ray Observatory) is an underground detector situated at the Gran Sasso Laboratory in Italy, at an average depth of 3700 meters of water equivalent (mwe) and a minimum depth of 3150 mwe. It uses three different types of detectors: liquid scintillators, limited streamer tubes and nuclear track detectors (CR39 and Lexan) disposed in a modular structure of six "supermodules" (SM's), each one subdivided in a lower and an upper part. The overall dimensions of the apparatus are $77 \times 12 \times 9$ m^3 (Ahlen et al., 1990). The response of the three types of detectors to slow and fast particles has been experimentally studied (Ficenec et al., 1987; Ahlen et al., 1983; Ambrosio et al., 1995; Baiocchi et al., 1995) .

One of the primary goals of MACRO is the search for superheavy GUT magnetic monopoles (Guarino et al., 1997). It was shown (Ahlen et al., 1992) that the monopole searches based on the liquid scintillator subdetector are sensitive also to nuclearites; in (Ambrosio et al., 1996) the response of the CR39 subdetector to nuclearites was analysed finding that it is efficient for any nuclearite with a velocity $\beta = v/c > 10^{-5}$. It was also shown that due to the low density of the filling gas, the limited streamer tube subdetector is not sensitive to nuclearites. Some earlier results of the search for strange quark matter in the penetrating cosmic radiation using the scintillator subsystem of one half of the lower part of the first MACRO module have been published (Ahlen et al., 1992).

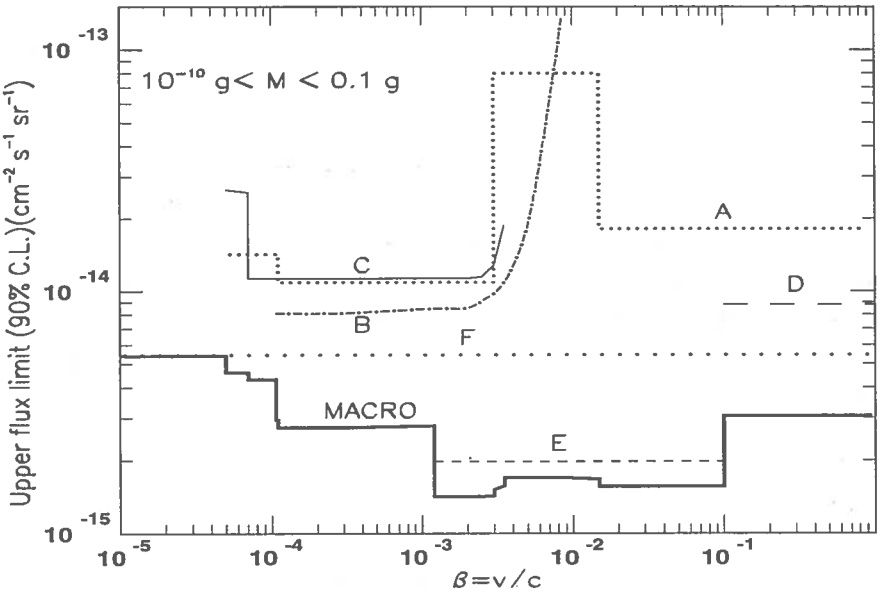

Figure 1: *90% C.L. MACRO limits for a flux of down-going nuclearites with masses of* $10^{-10} < M < 0.1g$. *See text for explanations.*

SEARCHES FOR NUCLEARITES WITH THE MACRO DETECTOR

Scintillators. It was shown that the scintillator sub-detector is sensitive to nuclearites with masses $M \leq 1.5$ ng having velocities as slow as $v = 5 \times 10^{-5}c$, (Ahlen et al., 1992) as the light yield should be above the 90%-trigger-efficiency thresholds of the scintillator slow-particle trigger system; thus the scintillators are sensitive not only to nuclearites of galactic or extragalactic origin, but also to those possibly trapped in our solar system. The nuclearite detection efficiency in the scintillation subdetector is assumed to be equal to that for magnetic monopoles. The analysis of the data collected during different periods of time during the completion of the detector and with the full detector did non find any nuclearite candidate; thus flux 90% C.L. upper limits could be established. Curves A - D in Figure 1 summarize for $M < 0.1$ g the limits for a flux of down-going nuclearites obtained during the construction phase; curve E refers to data collected also with the complete detector. For an isotropic flux of nuclearites ($M > 0.1$ g) the limits are lower by a factor of two and are shown in Figure 2. The limits A in Figures 1 and 2 were published in (S. Ahlen et al., 1992) while the other more recent limits in (Ambrosio et al., 1996).

CR39. For our CR39 the "intrinsic" threshold is about 20 MeV g^{-1} cm^2, in the condition of a chemical etching in 8 N NaOH water solution at 80° C. In order to reduce the background produced by neutron interactions, in the magnetic monopole searches the effective CR39 threshold was set at 50 MeV g^{-1} cm^2, by requiring the observation of traversing tracks with a diameter of at least 100 μm (Giacomelli et al., 1996).

The MACRO CR39 is sensitive to nuclearites of any mass and with $\beta > 10^{-5}$. As a consequence, the 90% C.L. limits for $\beta \sim 1$ monopoles established by the nuclear track sub-detector (2.2×10^{-15} cm^2 s^{-1} sr^{-1}) apply also to an isotropic flux of $M > 0.1$ g nuclearites. Lower mass nuclearites cannot traverse the earth; thus only nuclearites coming from above the detector are detected, the detection acceptance is half the previous value and the 90% C.L. flux limit is twice the previous value (4.4×10^{-15} cm^2 s^{-1} sr^{-1}) (Ambrosio et al., 1997). In the

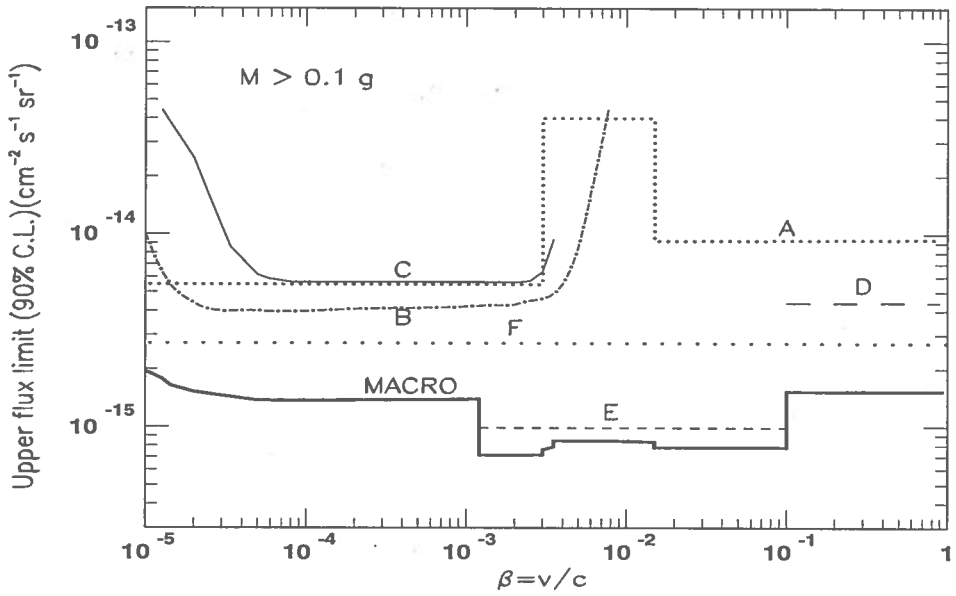

Figure 2: *90% C.L. MACRO limits for an isotropic flux of nuclearites with masses* $M > 0.1g$. *See text for explanations.*

case of nuclearites with masses lower than 1 μg and velocities $\beta = v/c$ between 10^{-5} and 10^{-4} there is an additional loss of acceptance (from few percents to about 50%) arrising from the limitation of the incidence angle for the formation of latent tracks in CR39. Those limits are presented in Figures 1 and 2 as curves *F*.

CONCLUSIONS

No nuclearite candidate was found in any of our searches. Assuming that either the scintillator or the CR39 analysis may rule out, within its own acceptance and sensitivity, a potential candidate from the other one, it follows that the present global MACRO limit for nuclearites may be taken as the "OR" combination of separate limits. Using a procedure based on the summation of the independent parts of the individual exposures, we obtain the corresponding global limit denoted as "MACRO" in Figures 1 and 2. This procedure ensures the 90 % C.L. significance of the global limits.

All limits presented in Figures 1 and 2 refer to the flux of nuclearites at the level of the MACRO detector, i.e. below an average rock thickness of 3700 hg cm^{-2}. In order to compare our limits with the limits published by different experiments and with the dark matter limit, we integrated the energy loss equation for a path corresponding to the averaged rock thickness and for different assumed velocity values at the detection level.

Figure 3 presents the MACRO global 90 % C.L. nuclearite flux limit assuming a nuclearite velocity at the detector level of $\beta = 2 \times 10^{-3}$. We include for comparison two other limits, from papers (Nakamura et al., 1991) and (Orito et al., 1991), obtained by experiments using the CR39 nuclear track detector; in (Nakamura et al., 1991) the experiment was performed at mountain altitude, while the experiment of reference (Orito et al., 1991), was performed at a depth of 100 mwe so the conditions that a nuclearite should fulfill in order to reach the detectors are different. These differences explain the different astrophysical limits computed for different experiments.

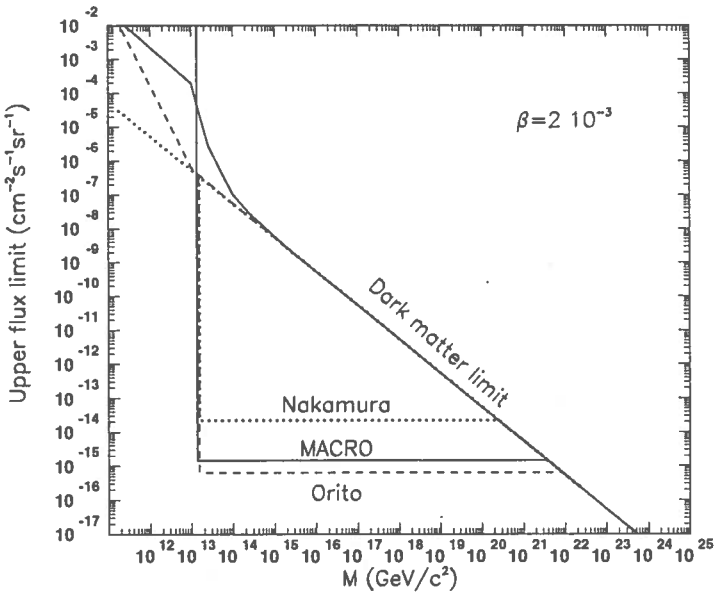

Figure 3: *90% C.L. MACRO global limit for a flux of down-going nuclearites, compared with other published limits and with the dark matter limit, assuming a nuclearite velocity of* $v = \beta c = 2 \times 10^{-3} c$.

REFERENCES

S. P. Ahlen and G. Tarlé, Phys. Rev. D**27** (1983) 688.
S. Ahlen et al. (MACRO Collaboration), Nucl. Instrum. Methods Phys. Res. A **264** (1990) 2094.
S. Ahlen et al., Phys. Rev. Lett **69** (1992) 1860.
M. Ambrosio et al. (MACRO Collaboration), Astrop. Phys. **4** (1995) 33.
M. Ambrosio et al. (MACRO Collaboration), MACRO/PUB 96/7 (1996).
M. Ambrosio et al. Astropart. Phys. **6** (1997) 113.
B. Baiocchi et al., Rad. Meas. **25** (1995) 145.
A. De Rújula, S. L. Glashow, Nature **312** (1984) 734.
D. J. Ficenec et al., Phys. Rev. D**36** (1987) 311.
G. Giacomelli et al. in Proc. of the 18th Int. Conf. on Nuclear Tracks in Solids, Cairo (1996).
F. Guarino et al. (MACRO Collaboration), in these Proceedings (1997).
S. Nakamura et al., Phys. Lett. B **263** (1991) 529.
S. Orito et al., Phys. Rev. Lett. **66** (1991) 1951.
E. Witten, Phys. Rev. D **30** (1984) 272.

THE MEASUREMENT OF THE ATMOSPHERIC MUON NEUTRINO FLUX USING MACRO

INFN/AE–97/21
19 Giugno 1997

ABSTRACT

The flux of muon neutrinos in the $1 - 1000\ GeV$ range has been measured with the MACRO underground detector. The measurement has been performed by means of the time-of-flight method to separate upward-going muons coming from neutrino interactions in the surrounding rock from downward-going muons coming directly from cosmic ray cascades. The data collected since March 1989 up to November 1996 are summarized. The zenith angular dependence of the measured upward-going muon flux is compared with the expected one assuming the Bartol atmospheric neutrino flux. Also upward-going muons generated inside the detector have been detected.

INTRODUCTION

Atmospheric neutrinos are produced in the cascade originated in the atmosphere by cosmic rays. A lower than expected ratio between atmospheric ν_μ and ν_e contained events has been measured by water Čerenkov experiments. This result has been seen as a clue of ν oscillation and the interest about precise measurements of the atmospheric neutrino flux increased in the last years.

The flux of ν_μ can be inferred from measurements of upward-going muons with underground detectors. The MACRO experiment (Ahlen et al., 1993), located in the Gran Sasso laboratory, is a proper tool for this measurement. The apparatus consists of 6 supermodules and has overall dimensions of $12 \times 77 \times 9\ m^3$. The bottom is filled with crushed rock absorber while the top is hollow (see Figure 1). The detection elements for muons are limited streamer chambers for tracking and liquid scintillator counters for fast timing. The intrinsic angular resolution is better than 0.5° and the time resolution is about $500\ ps$ for a single scintillator counter.

In MACRO the upward-going muon events due to interactions of ν_μ appear with three different topologies which are shown in Figure 1. Here we present the analysis of upward-throughgoing muon events, that is muons with enough energy ($E_\mu > 1\ GeV$) to cross the apparatus, produced in the rock outside the detector by ν_μ. The data collected in the period March 1989 - June 1993, when only lower parts of the apparatus were operative, have been already published (Ahlen et al., 1995). Now we present the data taken with the entire apparatus since April 1994 through November 1996 (life-time $\sim$ 2.2 years). The statistics of the new data set is $\sim$ 4 times higher than the previous one and the time measurement is better because the upper scintillator layers are now in data acquisition giving us three time measurements for throughgoing muons. Some preliminary results on partially contained muons produced by ν interactions (mean ν energy $\sim 2\ GeV$)

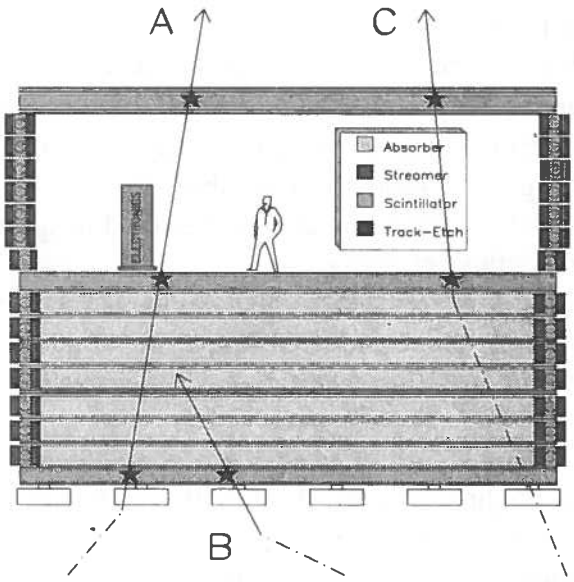

*Fig. 1: Cross section of the apparatus and topology of the upward-travelling tracks : (**A**) throughgoing, (**B**) stopping and (**C**) partially contained muons.*

inside the apparatus are also reported.

ANALYSIS PROCEDURE

The search for upward-going tracks is fully automated and based on the time-of-flight method. The fraction β of the light speed c is given by the following formula :

$$\frac{1}{\beta} = \frac{c \times (T_1 - T_2)}{L}, \quad (1)$$

where T_1 and T_2 are the times measured in the lower and in the higher scintillator planes, respectively, and L is the track length between the two scintillators. When the track hits three scintillator counters the time information is redundant and the β value can be calculated by means of a linear fit.

Looking at the $1/\beta$ value it is possible to get a rejection factor higher than the 10^6 necessary to separate a neutrino signal from muons directly produced by cosmic rays. In fact $1/\beta \simeq +1$ for particles going down through the detector and $1/\beta \simeq -1$ for upgoing particles. Some cuts have been used to remove background connected with radioactivity, stopping particles, multiple muons, showers and so on. A minimum path length ($2.5\ m$) assures that the time of flight is sufficiently larger than the time resolution of the scintillator system. Furthermore the geometrical agreement between streamer track and scintillator hits is required. An angular cut for nearly horizontal tracks has been necessary because the shape of the mountain permits cosmic ray muons to reach the detector from below in a well defined azimuth angle range. Furthermore a cut requiring the crossing of at least 200 g/cm^2 of material in the apparatus has been introduced to reduce the background discussed in another talk of this conference (Spurio et al., 1997) due to charged upgoing particles produced at large angles by downgoing muons. A contamination of ~ 1.5 % is expected to survive this cut.

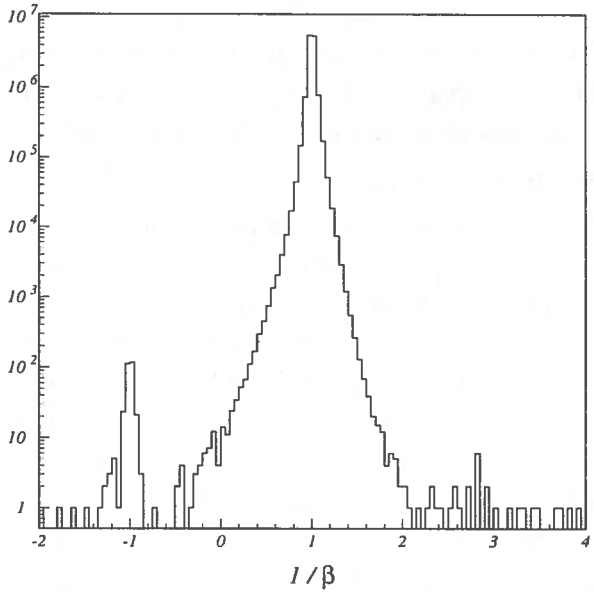

Fig. 2: $1/\beta$ distribution for throughgoing muons after the analysis cuts.

The $1/\beta$ distribution after all cuts is shown in Figure 2. Two well separated peaks indicate the signals from above and from below. In the range $-1.25 < 1/\beta < -0.75$, 286 upward-going muons are present, including an estimated background of ~ 4 events and the 1.5 % contamination previously quoted.

A new algorithm to search for partially contained tracks has been implemented. It is based on time-of-flight and on the check of the confinement of the interaction vertex in the detector. As a preliminary result 56 events have been found in the same data set here analyzed for throughgoing muons. In Figure 3 one of these events is shown. On the basis of Monte Carlo simulation ~ 89 % of them are expected to come from ν_μ charged current and ~ 11 % from ν_e and neutral current interactions.

SIMULATION

The simulation of the upward-going muon events has been performed assuming the Bartol neutrino flux (Frati et al., 1993; Agrawal et al., 1996), the muon energy loss calculated by Lohmann et al. (1985) for standard rock and the ν cross-section calculated by means of the Morfin and Tung parton distribution set S_1 (Morfin and Tung, 1991). The total error on the expected flux of muons at the detector due to uncertainties on these three quantities is ± 17 %.

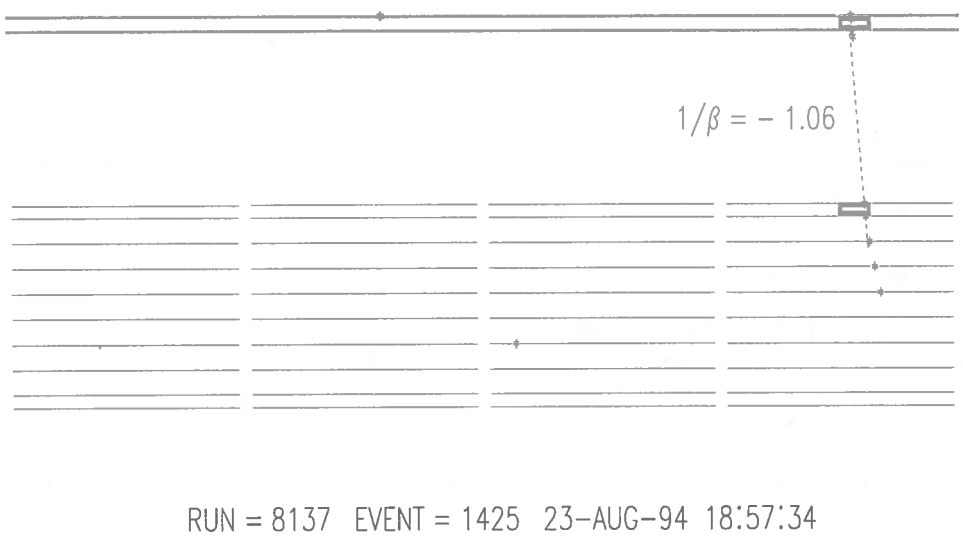

Fig. 3: An event with an upgoing muon generated by a neutrino interaction inside the apparatus. The rectangular boxes and the points indicate, respectively, scintillator counter and streamer tube hits. Only two supermodules of the apparatus are shown in one projective view.

The complete simulation of ν interaction and μ propagation in the rock surrounding MACRO has been implemented. The results of this new simulation do not differ from those of an older simulation in which the upgoing muons are simulated directly on the detector surface, in agreement with the analytically computed μ rate.

The apparatus and the data acquisition are fully reproduced in a GEANT (Brun et al., 1987) based Monte Carlo program and the simulated data are processed by means of the same automated analysis chain used for real data.

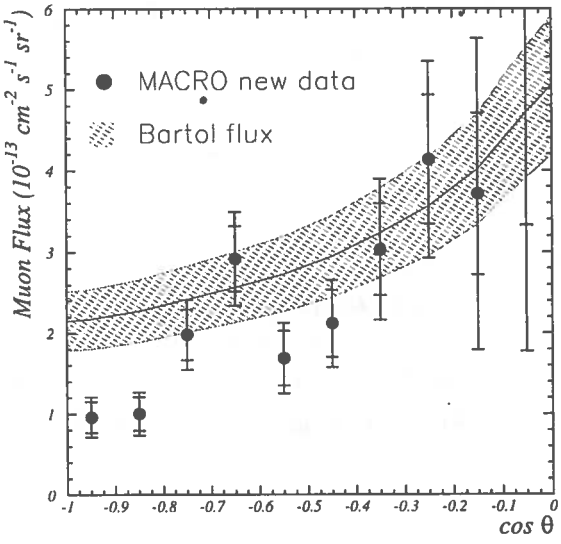

Fig. 4: Zenith distribution of the measured upgoing muon flux compared with the simulated one ($E_\mu > 1\ GeV$). Data : April 1994 - November 1996.

CONCLUSIONS

After the background subtraction the observed upward-throughgoing muons are $277 \pm 17_{stat} \pm 22_{syst}$. The 8 % systematic error is the sum of all acceptance errors and it has been evaluated by a thorough study of the downgoing muon sample. The expected number of events is $371 \pm 63_{theor}$. The ratio between observation and expectation is $0.75 \pm 0.05_{stat} \pm 0.06_{syst} \pm 0.13_{theor}$. Figure 4 shows the zenith angle distribution of the measured flux of upgoing muons compared with the expected one assuming an energy threshold of 1 GeV. Excluding the horizontal bin ($-0.1 < \cos\theta_{zenith}$) because of a possible contamination due to large angle scattering of downgoing

muons, the experimental points have been fitted with the expected flux assuming the normalization factor as a free parameter. The normalization factor results to be 0.75 with a χ^2 probability ~ 0.3 % (no ν oscillation assumed).

Taking into account also the published data (Ahlen et al., 1995) the results are not different. The ratio of the totals is $0.74 \pm 0.04_{stat} \pm 0.06_{syst} \pm 0.12_{theor}$. In Figure 5 the zenith angle distribution is shown for the entire MACRO data sample. The sum of the older and newer MACRO data does not modify significantly the shape of the observed flux.

We have to conclude that the total number of measured ν-induced muons may be compatible (8 % C. L.) with the expected number but the flux angular shape does not match the expectation. The deficit lies mainly in the vertical bins ($\cos\theta_{zenith} < -0.8$) just where the study of downgoing tracks reduces the uncertanties about the detector acceptance and efficiency. All checks performed on the downward-going muon data set confirm the accuracy of the claimed systematic errors. Different analysis approachs have been tested with the same results. On the other hand the distributions inferred from the $\nu_\mu \rightarrow \nu_\tau$ oscillation do not increase significantly the agreement between observed and calculated fluxes. More investigations about such a peculiar shape are necessary.

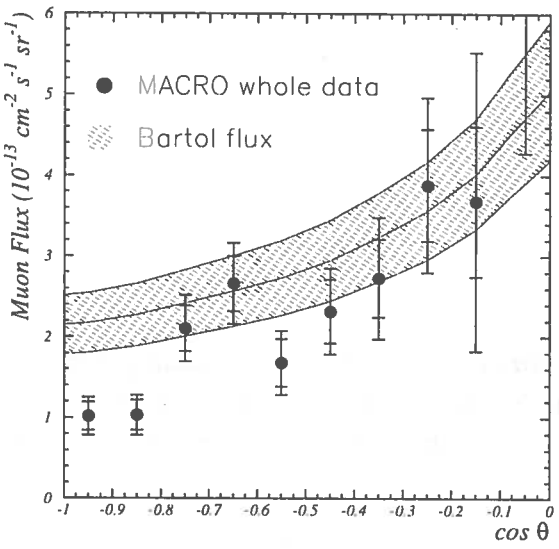

Fig. 5: Zenith distribution of the measured upgoing muon flux compared with the simulated one ($E_\mu > 1$ GeV). Data : March 1989 - November 1996.

REFERENCES

Agrawal, V. et al., *Phys. Review*, D 53, 1314 (1996).
Ahlen S. P. et al., MACRO Collaboration, *Nucl. Instr. Methods*, A 324, 337 (1993).
Ahlen S. P. et al., MACRO Collaboration, *Phys. Letters*, B 357, 481 (1995).
Brun, R. et al., CERN-DD/EE84-01 (1987).
Frati, W. et al., *Phys. Review*, D 48, 1140 (1993).
Lohmann, W. et al., CERN-EP/85-03 (1985).
Morfin, J.G., and Tung, W.K., *Zeit. Phys.*, C 52, 13 (1991).
Spurio M. (MACRO Collaboration), *Proc. 25th ICRC*, 4.1.13 (1997).

NEUTRINO ASTRONOMY WITH THE MACRO DETECTOR

INFN/AE–97/22
19 Giugno 1997

ABSTRACT

We present the results of a search for neutrino emission from point-like celestial objects and a search for coincidences with gamma ray bursts. For this search we used 605 upward-going muons produced by neutrino interactions in the rock below the MACRO detector in the underground Gran Sasso Laboratory.

INTRODUCTION

High energies neutrinos are expected to be emitted from a wide class of possible celestial objects: X-Ray binary systems, young supernova remnants , active galactic nuclei etc. (Gaisser, 1995). In the range of energies from several GeV to several TeV the detection of neutrinos is based on the observation of upward-going muons produced from neutrino interactions in the rock around the detector. Currently the expected signals are below the sensitivity of existing detectors. Only galactic supernovae are expected to give detectable signals after the supernova explosion. Several authors have also suggested a possible correlation between a gamma ray burst and emission of high energy neutrinos (Halzen, 1996) (Bahcall, 1997).

DATA SELECTION

The MACRO detector (Ahlen et al., 1993) located in the INFN Gran Sasso Laboratory consists of 6 supermodules and has overall dimensions of 12 m x 77 m x 9 m. The bottom half is filled with crushed rock while the top half is open. The detection elements for muons are planes of streamer tubes for tracking and liquid scintillators for fast timing. The angular resolution is better than 0.5°; the time resolution is about 500 psec. The angular resolution was checked with the moon shadow (Ambrosio et al., 1997a). Data for upgoing muons come primarily from three running periods and detector configurations: the lower half of the first supermodule from March 1989 through November 1991, the full lower half of the detector from December 1992 through June 1993 and the full detector from April 1994 until March 1997. Starting from August 1995 the apparatus is running in the final configuration.

The search for upgoing muons crossing the detector is done using the time-of-flight method and is described in detail in (Ambrosio et al.,1997b). In order to maximize the acceptance for this kind of search we do not require a minimum amount of material. Without this requirement we introduce some background due to large angle pions produced from downgoing muons (Ambrosio et al, 1997c) and we also add events with an interaction vertex inside the detector. We also included events which were observed during periods when the detector acceptance was changing with time due to construction work. All of these data can be used for the point source search since the benefit of the greater exposure in setting flux limits offsets the slight increase in the systematic error in the acceptance.

Figure 1 shows the $1/\beta$ distribution for the data set with full MACRO. The measured muon velocity is calculated with the convention that muons going down through the detector are expected to have $1/\beta$ near 1 while muons going up through the detector are expected to have $1/\beta$ near -1. Events with $-1.25 < 1/\beta < -.75$ are defined to be upgoing muon events. There are 605 events which satisfy this definition. Figure 2 shows the number of events as function of the year.

SEARCH FOR POINT LIKE SOURCES

A very important quantity in the search for point sources is the effective angular spread of the detected muon with respect to the neutrino direction. We computed the angle between the neutrino and the detected muon for several neutrino spectral indices γ. We assume a neutrino energy distribution like $dN/dE_\nu = constant \times E^{-\gamma}$ with a full Monte Carlo taking into account the neutrino-nucleon cross

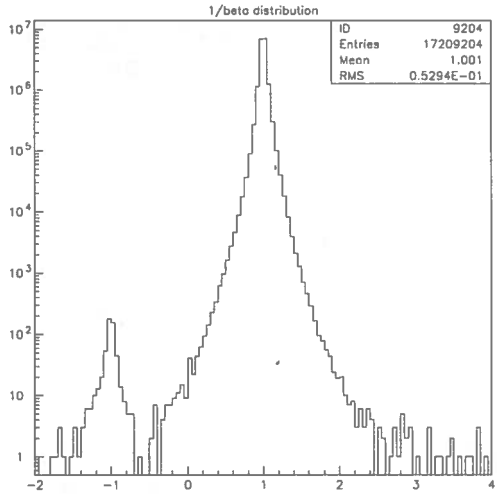

Fig. 1: The 1/β distribution

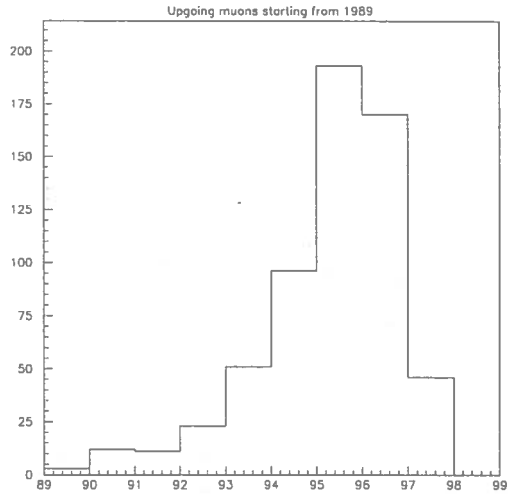

Fig. 2: Upward-going muon events versus year

sections, the muon energy loss in the rock and the detector angular resolution. Table 1 shows the fraction of events in a 3° search cone for two different neutrino spectral indices as a function of zenith angle.

Table 1: Fraction of events accepted in a 3° cone

Cos(Zenith)	$\gamma = 2$	$\gamma = 2.2$
0.15	0.77	0.72
0.35	0.90	0.85
0.55	0.91	0.87
0.75	0.91	0.87
0.95	0.91	0.87

Figure 3 shows the MACRO area as function of the zenith angle and Figure 4 shows the area averaged over 1 day as function of the declination of a possible source (this area includes the geometrical factors and the analysis cuts but does not include the reduction factor due to the search cone). The estimated systematic error is about 8% . In Table 2 are the results for several specific sources. The background was calculated from data itself, counting the events in a declination band of $\pm$ 5° around the declination of the source and having different right ascension. The limits were calculated including the reduction factor for a 3° search cone and spectral index $\gamma = 2.1$. The best limit from past experiments was taken from Baksan, IMB, Kamiokande, KGF (Gaisser, 1996). The neutrino flux limits were computed for a neutrino spectral index $\gamma = 2.1$ and with a threshold of 1 GeV on the neutrino energy. The MACRO data which we used are displayed in Figure 5.

To give an idea of the physical implications of those limits we recall that we expect from the supernova remnant Vela Pulsar (Gaisser, 1996) a muon flux of the order of 0.03 x 10^{-14}cm^{-2} s^{-1} (about one order of magnitude lower than the existing limits).

We also looked at the gamma ray sources listed in the Second Egret Catalog (Thompson, 1995). We found no statistically significant excess from any of the sources. We compared the results with the predictions obtained from a Monte Carlo simulation using the events themselves, changing randomly the association between times and angles (zenith, azimuth) and adding a smooth variation to the angles. We have found 5 sources with $\geq$ 2 events in the search cone to be compared to 8.4 sources expected

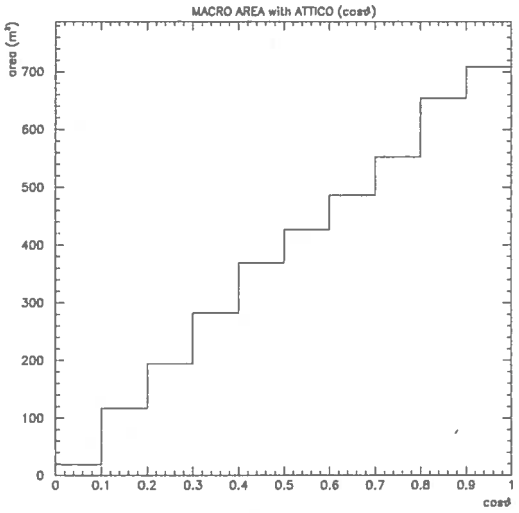

Fig. 3: Area as function of the zenith angle

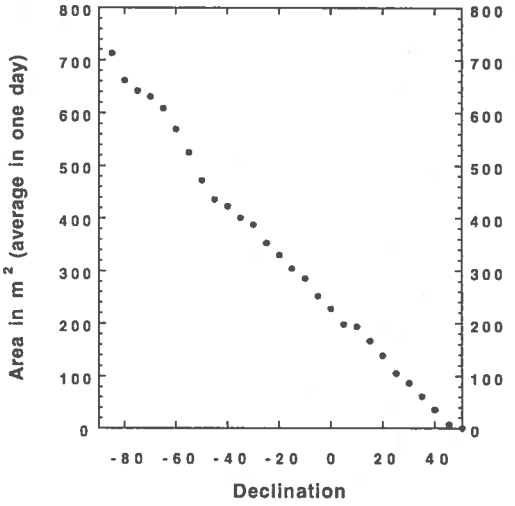

Fig. 4: Area as function of the declination

from the Monte Carlo.

We also looked for possible clusters of events counting the number of events in a 3° cone centered around a given event; we found 22 clusters of ≥ 3 events around a given event, to be compared with 21 expected from the Monte Carlo.

SEARCH FOR CORRELATION WITH GAMMA RAY BURSTS

We looked for correlations with the gamma ray bursts in the Batse Catalog 3b (Meegan, 1997) containing 1122 events in the time window between April 21th 1991 and September 19th 1994, overlapping with 143 upward-going muons collected from MACRO during this time. The area for upgoing muon detection in the direction of the bursts averaged over all the bursts in the catalog is $48m^2$; the number is small because MACRO is sensitive to neutrinos in only one hemisphere and because MACRO was not completed in the period between 1991-1994. We found no statistically significant correlation between neutrino events and gamma bursts. We particularly looked in a search cone of 20° around the gamma burst direction (determined from the Batse angular accuracy) and in a time window of ± 200 sec: we found no events, compared with 0.33 expected from the background. The expected value was computed with the delayed coincidence technique. The corresponding upper limit at 90% C. L. is 3.9 $\times\ 10^{-9}\mathrm{cm}^{-2}$ upward-going muons per burst. This limit is almost five orders of magnitude lower than the flux of the "extreme" topological defects model reported in (Halzen, 1996).

REFERENCES

Ahlen, S. P. et al., MACRO Collaboration, Nuclear Instruments Methods A324 337 (1993)
Ambrosio, M. et al., MACRO Collaboration, Phys Lett B357, 481 (1995)
Ambrosio, M. et al., MACRO Collaboration, paper HE 3.1.17 at this conference (1997a)
Ambrosio, M. et al., MACRO Collaboration, paper HE 4.1.14 at this conference (1997b)
Ambrosio, M. et al., MACRO Collaboration, paper HE 4.1.13 at this conference (1997c)
Bahcall, J. and Waxman, E., Phys Rev Lett 78 2292 (1997)
Gaisser, T. K., Halzen, F. and Stanev, T. Physics Reports 258 (1995) 173
Gaisser, T. K. Nucl Phys B (Proc Suppl) 48 (1996) 405
Halzen, F. and Jaczko Phys Rev D54 2779 (1996)
Meegan, C. A. et al http://www.batse.msfc.nasa.gov/data/3bcatalog (1997)
Thompson, D.J.et al http://cossc.gsfc.nasa.gov/cossc/egret/egretcatalog and Astr Journ. Suppl. (1995)

Table 2: Limits for Selected Sources at 90% CL. Muon flux limits in unit 10^{-14}cm^{-2} s^{-1}. Neutrino flux limits in unit 10^{-5}cm^{-2} s^{-1}

Source	δ	Events in 3°	Background	Muon flux limit	Old best limit (muons)	Neutrino flux limit
Cyg X-3	40.8	0	0.06	9.9	4.1 Baksan	5
MRK 421	38.1	0	0.07	9.1	3.3 IMB	4.6
Her X-1	35.4	0	0.14	6.4	4.3 IMB	3.2
Crab Nebula	22	1	0.25	3.8	2.6 Baksan	1.9
Geminga	17.8	0	0.21	2.1	3.1 IMB	1
SS433	5	0	0.34	1.4	1.8 Baksan	0.72
Sco X-1	-15.6	1	0.47	1.57	1.5 Baksan	0.78
Kepler 1604	-21.5	2	0.51	1.92	-	0.96
Galact Cent	-28.8	0	0.5	0.76	0.95 Baksan	0.37
Vela XR-1	-40.5	0	0.65	0.67	0.45 Baksan	0.33
SN 1006	-41.7	1	0.66	1.12	-	0.56
Vela pulsar	-45.3	0	0.76	0.64	0.78 IMB	0.32
CEN XR-3	-60.6	1	1.04	0.84	0.98 IMB	0.42
LMCX-4	-66.4	0	1.15	0.46	0.36 Baksan	0.23
SN1987 A	-69.4	0	1.1	0.46	1.15 Baksan	0.23

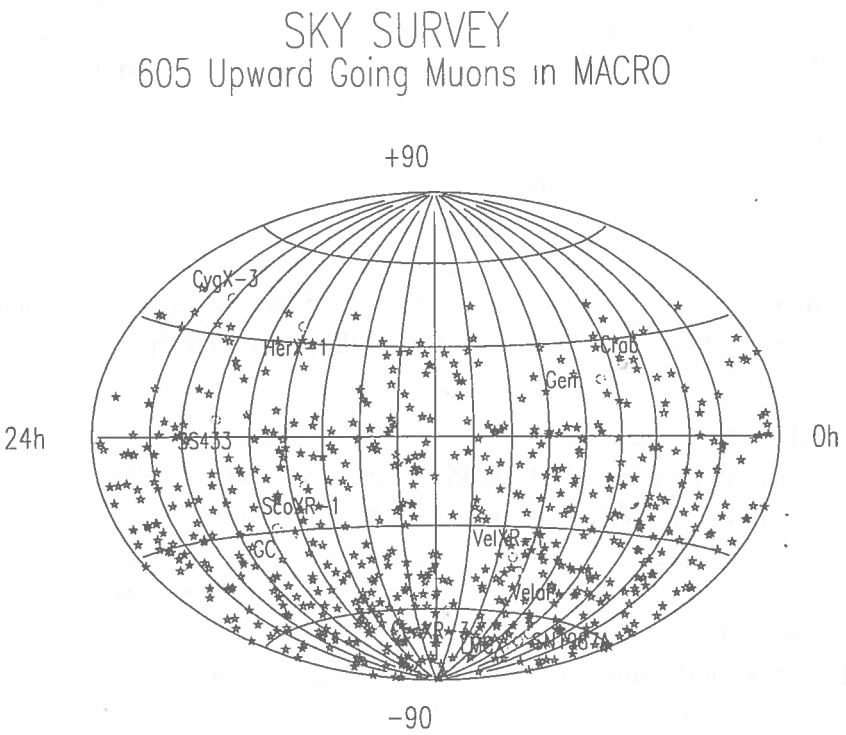

Fig. 5: Upgoing muon distribution in equatorial coordinates.

INDIRECT SEARCH FOR WIMPS WITH THE MACRO DETECTOR

INFN/AE–97/23
19 Giugno 1997

ABSTRACT

High energy neutrinos have been indirectly measured as upward-going muons in the MACRO detector using the time-of-flight technique. No statistically significant excess from the direction of the Earth and of the Sun have been found comparing the 364 measured upgoing muons to the expected background due to atmospheric neutrinos. Muon flux limits are given in arbitrary search cones and as a function of the neutralino mass.

INTRODUCTION

There are enough hints to suggest the existence in our Universe of a non-baryonic dark matter such as the *Weakly Interacting Massive Particles*. The luminous matter in galaxies, in fact, contributes less than 1% to the overall density of the Universe. Considerations on the structure formation and limits on the baryonic content of the Universe from Big Bang nucleosynthesis together with the aesthetical $\Omega = 1$ from inflationary theories have led to a wide list of Cold Dark Matter candidates (Jungman et al., 1996). Among them the most promising one is the neutralino, which is the Lightest Supersymmetric Particle in large regions of the supersymmetric space of parameters. In the Minimal Supersymmetric Standard Model the four neutralino mass states $\tilde{\chi}_i^0$ are linear superpositions of gaugino and Higgsino eigenstates. Their masses depend on the gauge fermion masses at the electroweak scale M_1 and M_2, on the Higgsino mass parameter μ and on the ratio of the Higgs doublet vacuum expectation values $\tan\beta$.

The lower limit on neutralino mass m_χ resulting from combined LEP 1 ($\sqrt{s} \sim M_Z$) and LEP 1.5 ($\sqrt{s}$ = 130 - 136 GeV) data, although model dependent and connected with the limits from chargino searches, exclude a lightest neutralino with mass less than 12.8 GeV/c^2. This limit rises to 34.1 GeV/c^2 for large $\tan\beta$ values when the sneutrino mass is greater than 200 GeV/c^2 (Buskulic et al., 1996). Moreover, combining the cosmological constraint on $\Omega_\chi h^2$ with the assumption of radiative electroweak symmetry breaking strengthens the lower limit in the case of $\mu < 0$ to 21.4 GeV for low $\tan\beta$ and to 51 GeV for $\tan\beta > 5$; in the case of $\mu > 0$ to $m_\chi > 56$ GeV for $\tan\beta < 3$ and $m_\chi > 36$ GeV for $\tan\beta < 3$ (for large sneutrino masses) (Ellis et al., 1996).

In this picture, the direct and indirect methods of detection mainly performed in underground detectors can probe complementary regions of the supersymmetric parameter space even when LEP 2 results will be available. Direct methods employ low-background detectors (e.g. semiconductors or scintillators) to measure the energy deposited when a WIMP elastically scatters from a nucleus therein. On the other hand, there are good prospects for indirect detection of neutralinos due to high energy ν radiation from WIMP annihilation in the core of the Earth and of the Sun.

THE INDIRECT SEARCH: THE MEASUREMENT OF UPGOING MUONS IN MACRO

Halo WIMPs can lose enough energy to become gravitationally trapped in the core of celestial bodies through elastic scattering in the nuclei therein. While their density builds up inside the body, their annihilation rate increases until equilibrium is achieved between capture and annihilation. High energy neutrinos are eventually produced via the hadronization and/or decay of the annihilation products (mostly fermion-antifermion pairs, weak and Higgs bosons) and can be detected as upward-going muons in underground detectors. The more the upgoing muon follows the parent direction, i. e. the higher the WIMP mass, the better the signal to noise ratio. The signal from WIMP annihilation should

be discriminated as a statistically significant excess of events in the direction of the Sun or of the Earth among the background of atmospheric neutrino induced upgoing muons. Data on upward muons from the core of the Earth and of the Sun have been measured by several experiments, notably Baksan (Boliev et al., 1996), MACRO (Ambrosio et al., 1996), Kamiokande (Mori et al., 1993), IMB (Losecco et al., 1987) and Frejus (Arpesella et al., 1988).

The MACRO detector (Ahlen et al., 1993), located in the INFN Gran Sasso Laboratory, measures upgoing muons using a system of streamer tubes for tracking (angular resolution $\sim 0.5°$) and liquid scintillator counters for fast timing (time resolution ~ 500 psec) with overall dimensions of 12 m $\times$ 77 m $\times$ 9 m. The bottom part of the apparatus is filled with rock absorber which sets a minimum threshold of about 1 GeV for vertical muons crossing the detector. Roughly 16 million muons from about 1.4 yr of running with 1/6 of the lower detector (Mar. '89 - Nov. '91) combined with 6 months of running of the lower detector (Dec. '92 - Jun. '93) and with 2 yr of running of the full detector (Mar. '94 - Nov. '96) have been analyzed looking for upward-going muons. The results of the lower detector upgoing muon analysis have been published (Ahlen et al., 1995) and updated (Ambrosio et al., 1997).

THE SEARCH FOR A WIMP SIGNAL FROM THE EARTH AND THE SUN

We use the sample of 364 events selected in the upgoing muon analysis (Ambrosio et al., 1997).

The background to an astrophysical source of neutrinos is due to atmospheric neutrinos. We have evaluated this background using a Monte Carlo calculation we described previously (Ahlen et al., 1995).

In the case of the Sun, the times from real downgoing muons measured during data taking have been given randomly to the simulated events to evaluate their right ascension, hence taking into account drifts of detection efficiency in time. Fig. 1 shows the angular distribution of the upgoing muon events with respect to the direction of the Sun compared to the expected one from atmospheric neutrinos. The simulated distribution has been normalized by a factor of 0.765, the ratio of the events detected and expected outside the region interesting for the signal (30° from the direction of the Sun). The shape of this distribution depends on the seasonal variation of the position of the Sun with respect to the apparatus and on the livetime of the apparatus.

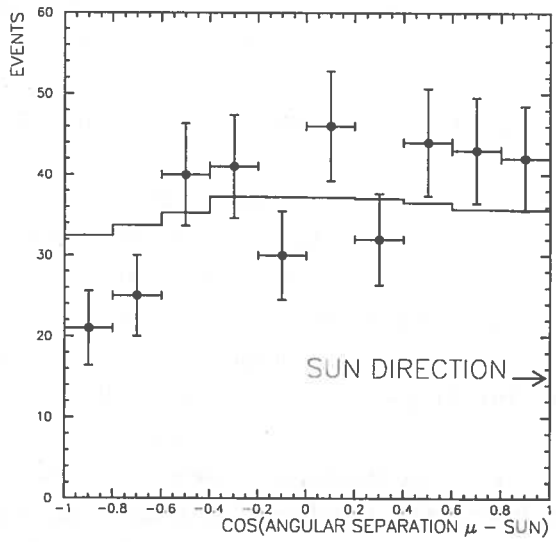

Fig. 1: Distribution of the cosine of the angular separation of upgoing muon events and the Sun position for the data and the normalized simulation.

The exposure of the Sun has been calculated as:

$$exposure = \int_{T_{start}}^{T_{end}} \epsilon \times A(\Omega(t))dt \qquad (1)$$

where A(Ω(t)) is the detector area in the direction Ω of the Sun at time t (set to zero when the Sun is below the horizon), ϵ is the detector efficiency, T_{start} and T_{end} are the beginning and the end times of the data taking. Tab. 1 shows the number of events detected and expected inside 6 arbitrary cones around the direction of the vertical of the apparatus and of the Sun. The 2 GeV threshold energy for the Sun corresponds to the value at which the area of the apparatus seen by the Sun becomes independent of energy. In the case of the Earth the threshold energy is 1.5 GeV because tracks are less slanted.

Due to the deficit of the measured events with respect to the predicted upgoing events induced by the atmospheric neutrino background near the vertical of the apparatus (Ambrosio et al., 1997), we give conservative flux limits for the Earth assuming that the number of events measured equals the number of events expected (Barnett et al., 1996).

Table 1: Selected and expected events and 90% C.L. muon flux limits for 6 cones around the Earth and Sun directions.

	EARTH			SUN		
Cone	Data	Background	Flux Limit $(E_\mu > 1.5GeV)$ $(cm^{-2}s^{-1})$ Exp. = 1900 m^2yr	Data	Background	Flux Limit $(E_\mu > 2GeV)$ $(cm^{-2}s^{-1})$ Exp. = 480m^2yr
30°	48	87.2	2.67×10^{-14}	30	23.9	9.74×10^{-14}
25°	36	61.9	2.14×10^{-14}	18	16.7	6.04×10^{-14}
20°	23	40.2	1.72×10^{-14}	12	10.4	5.35×10^{-14}
15°	16	22.7	1.44×10^{-14}	3	6.0	2.30×10^{-14}
10°	7	10.2	1.08×10^{-14}	1	2.6	1.91×10^{-14}
5°	1	2.7	5.98×10^{-15}	1	0.7	2.26×10^{-14}

Flux limits from the study of the angular distributions

The signal of upgoing muons produced by WIMP annihilation has an angular shape that is due to several sources. As the diameter of the Sun is about 0.5° large as viewed from the Earth, the difference in angle between the center and the border of the annihilation region can be totally neglected with respect to other spreading effects. The induced muons are distributed around the neutrino direction because of the $\nu - \mu$ angle due to ν CC-interaction in the Earth and of the multiple scattering of muons in the path from the neutrino interaction point to the detector. The distribution of the $\nu - \mu$ angle is of course dependent on the shape of the neutrino energy spectrum. The energy spectrum of neutrinos produced in the annihilation of a WIMP of mass m_χ depends in principle on the details of the final states produced in the annihilation. However, the most important parameter in determining the shape of the spectrum is simply the neutralino mass, which sets the maximum neutrino energy $E_{max} = m_\chi$. In fact, the dependence of the angular spread of the muon signal on other model parameters is of the order of 1°.

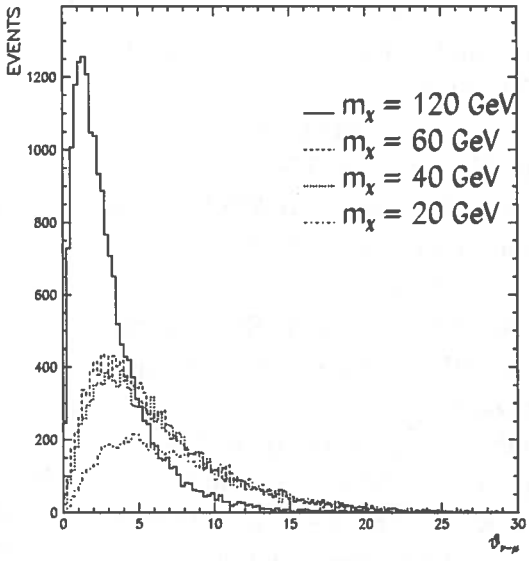

Fig. 2: Angle between the direction of the parent neutrino fron χ annihilation in the Sun and the generated muon direction for different neutralino masses.

The shape of the upgoing-muon signal using neutrino fluxes from χ annihilation in the Sun calculated by Bottino et al. (Bottino et al., 1995) has been evaluated and it is shown in Fig 2. The neutrino fluxes induced by 20, 40, 60 and 120 GeV neutralinos with fixed sets of model parameters and maximal mixing have been used as input to a Monte Carlo which uses the cross sections described in (Lipari et al., 1995) and propagates the muon to the detector treating the energy loss as described in (Lipari and Stanev, 1991). The 90% C.L. flux limits have been calculated in neutralino mass depen-

dent windows which collect 90% of the signal from the Sun (respectively 16.0°, 13.8°, 13.2° and 7.6° for $m_\chi = 20, 40, 60, 120$ GeV). The results are illustrated in Fig. 3 where the muon flux limits have been superimposed to the flux of upgoing muons from the Bottino et al. calculation as a function of m_χ.

In order to increase the sensitivity of this search, an optimization of the signal to noise ratio has been performed. The data, signal, and background angular distributions have been fitted in the region interesting for the signal using a χ^2 expression suited for Poisson-distributed data in counting experiments (Barnett et al., 1996). In this χ^2, the signal is multiplied by a factor K. The normalization factor K of the signal is found by minimizing the χ^2 with respect to K. The resulting flux limits, shown in Fig. 3 (solid curve), have been evaluated at the 90 % C.L. as a function of the neutralino χ mass. This method is more correct than choosing *a priori* the search cone and it will certainly be improved with increasing statistics.

CONCLUSIONS

The search for a WIMP signal has been performed on the full MACRO through-going upgoing muon sample with negative results. The increased statistics and exposure have made MACRO flux limits more significant than other published results.

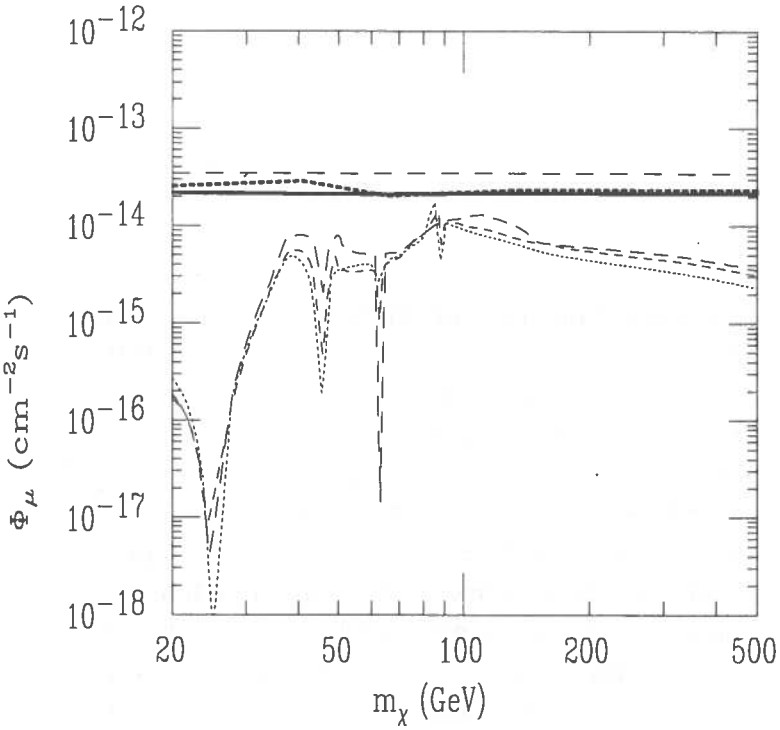

Fig. 3: The bottom three curves are predicted upgoing muon fluxes from the Sun (Bottino et al., 1995). The dotted line connects MACRO flux limits in windows containing 90% of the signal for different m_χ masses. The solid line is described in the text. The dashed line is Baksan flux limit (Boliev et al., 1996).

REFERENCES

Ahlen, S. P. et al., MACRO Collaboration, *Nucl. Inst. and Meth. A* **324**, 337 (1993).

Ahlen, S. P. et al., MACRO Collaboration, *Phys. Lett. B* **357**, 481 (1995).

Ambrosio M. et al., MACRO Collaboration, *Nucl. Phys. B* (Proc. Suppl.) **48**, 87 (1996).

Ambrosio, M. et al., MACRO Collaboration, HE 4.1.14 at this conference (1997).

Arpesella, C. et al., Proc. of the XXIIIrd Rencontre de Moriond (1988).

Barnett, R. M. et al., Review of Particle Physics, *Phys. Rev. D* **54** (1996).

Boliev, M. M. et al., *Nucl. Phys. B* (Proc. Suppl.) **48**, 83 (1996).

Bottino, A., Fornengo, N., Mignola, G., Moscoso, L., *Astroparticle Physics* **3**, 65 (1995).

Buskulic, D. et al., *Z. Phys. C* **72**, 549 (1996).

Ellis, J. et al., *Phys. Lett. B* **388**, 97 (1996).

Jungman, G., Kamionkowski, M. and Griest, K., *Phys. Rep.*, **267**, 1955 (1996).

Lipari, P., Lusignoli, M., Sartogo, F., *Phys. Rev. Lett.* **74**, 4384 (1995).

Lipari, P. and Stanev, T., *Phys. Rev. D* **44**, 3543 (1991).

Losecco, J. M. et al., *Phys. Lett. B* **188**, 388 (1987).

Mori, M. et al., *Phys. Rev. D* **48**, 5505 (1993).

OBSERVATION OF UPGOING CHARGED PARTICLES IN MACRO PRODUCED BY HIGH ENERGY INTERACTIONS OF MUONS

INFN/AE-97/24
19 Giugno 1997

ABSTRACT

The experimental study of upgoing charged particles produced underground by hard muon scattering has been studied by the MACRO experiment at the Gran Sasso Laboratory. At total of 243 events with an upgoing particle associated with a downgoing muon in a sample of 12.2×10^6 single muons were found. These events may represent a source of background for the measurements of the muon neutrino flux using upward throughgoing and stopping muons. The implications for MACRO as a muon neutrino detector are discussed.

INTRODUCTION

Upgoing particles (which most likely are charged pions) induced by the hard muon scattering on a nucleon N, $\mu + N \rightarrow \mu + \pi^{\pm} + X$, have been detected by the MACRO experiment at the the Gran Sasso depth. These events have never been previously observed in underground experiments. A data taking periods of $1.55\ y$ was considered; during this period, $12.2\ 10^6$ single downgoing muons and 243 events with upgoing charged particles associated with a downgoing muon were detected. The distributions of the pion range, of the emission angles with respect to the muon direction and of the distance between the downgoing muon and the upgoing pion have been measured.

If the downgoing muon is not detected (for example when the μ passes near but not through the detector) the upgoing pion induced by the muon simulates an upgoing neutrino-induced muon. This represents a background for the flux measurement of neutrino-induced upward throughgoing and stopping muons, which is evaluated for our detector in the last section.

MUON-INDUCED UPGOING PARTICLES IN MACRO

The MACRO detector (Ahlen et al., 1993) consists of a large rectangular box divided in six equivalent parts called supermodules, with overall dimensions of $77m \times 12m \times 9m$. The detection elements are planes of limited streamer tubes for particle tracking and liquid scintillation counters for fast timing. The directions of throughgoing particles in the detector are determined by time-of-flight with scintillator. Vertical muons crossing MACRO pass through $\sim 500\ g/cm^2$ of MACRO material (absorber plus active elements), corresponding to a minimum threshold energy of about $1\ GeV$ for muons.

High energy secondaries produced at large angles by muon interactions in the rock or in the concrete below the apparatus are identified using the tracking system. The topology of such events is that of two tracks converging somewhere below the detector, both in the wire and strip projective views of the tracking system (see Figure 1). A dedicated tracking algorithm was developed to reconstruct the upgoing short tracks in events in which a single downgoing muon is already present; for a description of the standard tracking algorithm, see (Ahlen et al., 1993). Any alignment between at least three hits (including the scintillator hit) was considered a track. The minimum pion vertical depth for events reconstructed in such a way is $\sim 30\ g\ cm^{-2}$. Timing information from the scintillation counters is used to identify the direction of the two particles.

Data corresponding to a detector livetime of $1.55\ y$ were analyzed; in this period, $12.2\ 10^6$ single downgoing muons were collected. Upgoing pions induced by downward going muons were searched for in double track events in which one of the two tracks has been reconstructed by the dedicated tracking algorithm. In the most common case (71%) the short track in the event belongs to a second down-

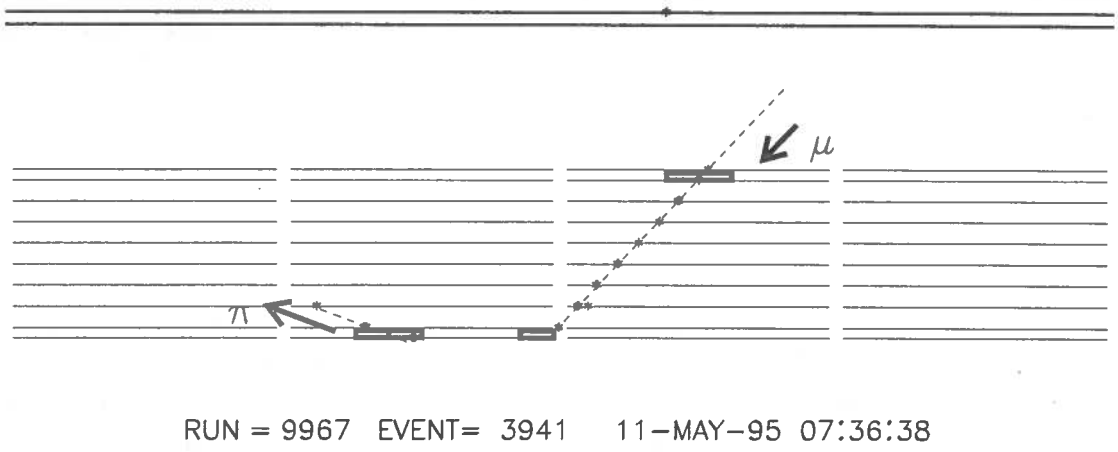

Fig. 1: On-line display of a typical muon interaction in the rock below the apparatus giving rise to an upgoing charged particle. The muon is coming from the lateral wall of the upper part.The rectangular boxes indicate scintillator counters hits and the points are streamer tube hits. The tracks are reconstructed in the wire view of the streamer tubes, and only two supermodules (24m) are shown.

going muon, parallel to the first one. Other cases giving a fake short track are electromagnetic showers of muons inside the detector (17%), bad tracking results (4%), muon interactions occurring inside the detector (5%) and low momentum muons with a curved trajectory (2%). A sample of 243 events with an upgoing track associated with a muon interaction were found. Four of them have both particles tracked by the standard tracking algorithm. The identification relies on the event topology from tracking and on the timing information from scintillator, and was performed using software cuts and a visual scan with the MACRO event display. A selection efficiency $\epsilon_s = (95 \pm 2)\%$ was estimated using a simulated sample of events, as described in the next section.

ANALYSIS OF THE UPGOING PARTICLES

The distributions presented in Figure 2 were obtained using the results of the track fitting procedure from the 243 selected events. They refer to: *(i)* the range of the upgoing particle (total and inside the detector); *(ii)* the scattering angles between the downgoing and the upgoing particles; and *(iii)* the distribution of the radial distance D between the upgoing π and the downgoing μ. The total range of the upgoing particle is calculated from the estimated interaction point (vertex) up to the stopping point inside the detector. The distribution and density of the material inside and around the apparatus as included in the reconstruction programs was used. The vertex lies below the detector, and corresponds to the intersection point of the two reconstructed tracks (see Figure 1) in the two views of the tracking system. If the value of the vertex depth in the two views differs by less than 50 cm, the event is defined as well reconstructed. For the well reconstructed subsample (168/243 events), the total range of upgoing particles is presented in Figure 2a. For the remaining 75 events, the uncertainty on the total range is at least of $\sim 100\ g\ cm^{-2}$.

The partial range of the upgoing particle inside the apparatus is calculated from the entry point up to the stopping point and is presented in Figure 2b (all events were included). Figure 2c shows the measured distribution of the scattering angle $\Delta\alpha$ of the pion with respect to the muon direction in the zenith plane; Figure 2d shows the distribution of the distance D between the muon and the upgoing pion at $z = 89\ cm$, the center of the bottom layer of the scintillator counters. The distributions fall for small D and $\Delta\alpha$ is due to a low reconstruction efficiency. The radial distance between the two tracks is less than $4\ m$ (about one third of the dimension of one MACRO supermodule) in 90% of the cases. The distributions presented in Figure 2 allows to estimate the probability that a muon-induced upgoing pion gives a background event for the ν_μ studies, as discussed in the last section.

The detection of an upgoing pion produced at a certain point below the detector by a downgoing muon depends on the muon angular distribution at the MACRO location, on the emission angles of

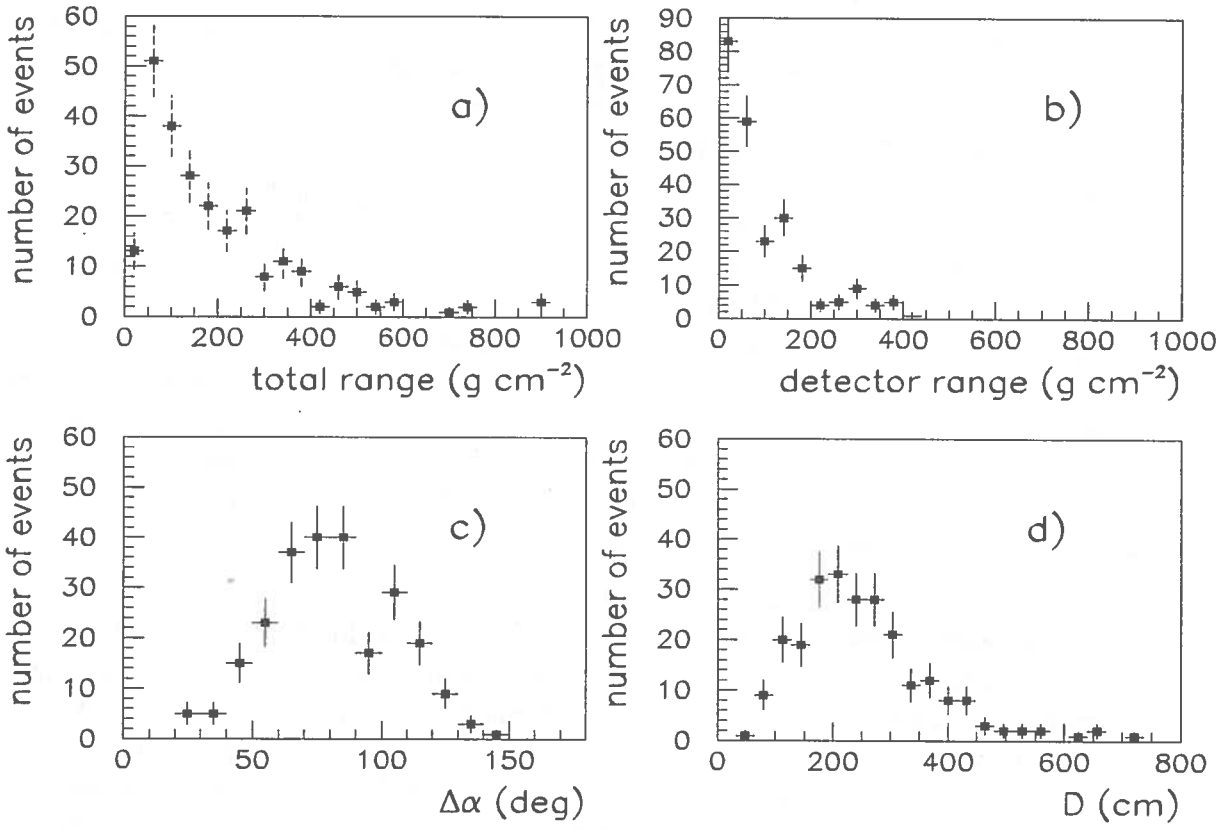

Fig. 2: a) Distribution of the reconstructed total range crossed by upgoing particles with a well reconstructed interaction vertex (168 well reconstructed events). b) Distribution of the reconstructed detector range crossed by the upgoing particles. c) Measured distribution of the $\pi - \mu$ scattering angle $\Delta\alpha$ and d) of the distance D between the downgoing muon and the upgoing pion at the z location of the centre of the bottom layer of scintillation counters. All events were included in b),c) and d).

the pion with respect to the muon and on the pion range. The probability to detect a muon-pion pair in MACRO for different values of these parameters was evaluated using a Monte Carlo. This allows the calculation of the reconstruction efficiency ϵ_r for these events. The probability to detect and reconstruct both the muon and the upgoing pion is less than 5% if the scattering angle $\Delta\alpha < 45^o$ (i.e. when both the pion and the muon are near-horizontal in the MACRO reference frame) (see Figure 2c); the tracking efficiency is small for $D < 100$ cm (Figure 2d) because the tracking algorithm do not discriminate the pion and the muon tracks if they are too near. The reconstruction efficiency, for $\Delta\alpha > 45^o$ and averaged over the remaining parameters quoted above, is $\epsilon_r = (21 \pm 2_{stat} \pm 4_{sys})\%$.

From the detected number of events, the selection efficiency ϵ_s and the detection probability ϵ_r, the detector-independent number of upgoing pions per downgoing muon emerging from the floor at the MACRO depth and with a scattering angle in the zenithal plane $\Delta\alpha > 45^o$ was estimated as

$$N_{\pi/\mu} = \frac{243}{(\epsilon_s \times \epsilon_r) \times 12.2\ 10^6} = (10^{+4}_{-2.5})\ 10^{-5}$$

COMPARISON WITH A MODEL OF H.E. MUON INTERACTIONS

Preliminary estimates of pion production by underground muons in MACRO have been made with a stand-alone full simulation with FLUKA (Fassó et al.,1993), interfaced with a simplified version of the apparatus response. The FLUKA code uses a model of hard muon scattering with the muon photonuclear cross sections (Bezrukov and Bugaev, 1981); at the MACRO depth, the cross sections

for the average muon energy is $\sigma_\gamma(\overline{E}_\mu = 300\ GeV) \simeq 0.40\ mb$.

To evaluate the number of events in MACRO with an upgoing pion induced from this process by a downgoing muon, the atmospheric muon spectrum at the MACRO location, and the differential yield $Y_{\pi/\mu}$ of charged pions are needed. The measured angular distribution (Ambrosio et al., 1995) of the survived atmospheric muons (after the unfolding of the detector acceptance) was used; the muon energy is extracted between 1 GeV up to 10 TeV following the analytic approximation model (Gaisser, 1990) for the muon energy spectrum at a depth of $h = 3.8\ km.w.e.$. The muons interact randomly below the detector, and the energy spectrum of the upgoing particles from the floor is evaluated. It was found that the charged particle yield is dominated by charged pions; the charged kaon contribution is lower by about one order of magnitude. Protons (and neutrons) have an energy spectrum considerably softer than that of pions. The pion yield decreases sharply with increasing pion kinetic energy. For this reason, we identify the upgoing particles with charged pions. The number of upgoing pions per downgoing muon is calculated integrating the yield $Y_{\pi/\mu}$ of charged pions emerging from the floor over the differential energy and angular distribution. With this calculation, we find $(11.5 \pm 4.5)\ 10^{-5}$. This number agrees well with the experimental value $N_{\pi/\mu} = (10^{+4}_{-2.5})\ 10^{-5}$

BACKGROUND FOR MUON NEUTRINO STUDIES

The flux of atmospheric muon neutrinos $\Phi_{\nu(\mu)}$ at the Gran Sasso location can be inferred from the measurement of upgoing muons. The probability that a downgoing muon misses the apparatus while an upgoing pion is observed, simulating an upgoing muon, was evaluated using a simulation whose input data are the measured distributions corrected for the detector detection probability. Upgoing pions crossing two scintillator planes and at least 200 $g\ cm^{-2}$ of detector material represent the background for the measurement of upward throughgoing muons (Ambrosio et al., 1996). The estimated background rate is $(1.9 \pm 0.5_{stat} \pm 0.4_{sys})\ events/year$ for the upward throughgoing sample for a muon energy threshold of $\sim$ 400 MeV. If the upgoing pion stops inside the *fiducial volume* defined in (Mikheyev, 1994) an upgoing stopping muon is simulated. The estimated background rate is $(5.9 \pm 0.9_{stat} \pm 0.6_{sys})\ events/year$ for the upgoing stopping sample. This background is of the order of $\sim 1\%$ of the upward throughgoing muons and of the order of 8% of the upgoing stopping muons. The quoted background is specifically evaluated for MACRO. The probability to detect the pion and to miss the muon increases for smaller and shallower detectors.

REFERENCES

Ahlen, S. P. et al., MACRO Collaboration, Nucl. Inst. and Meth. **A324**,337 (1993) .

Ambrosio M. et al., MACRO Collaboration, Phys.Rev. **52D**,3793(1995) .

Ambrosio, M. et al., MACRO Collaboration, (Neutrino results using upward-going muons in MACRO), MACRO/PUB 96/4 (1996).

Bezrukov, L. B. and Bugaev, E. V., Sov. J. Nucl. Phys. 33,635(1981).

Fassó, A. et al., (FLUKA: present status and future developments), *Proc. of the IV Int. Conf. on Calorimetry in High Energy Physics,* La Biodola (Is. d'Elba), Italy, (ed. World Scientific),493(1993).

Gaisser, T. K., Cosmic Rays and Particle Physics, Cambridge University Press, Cambridge, England (1990).

Mikheyev, S. P., (Detection of High Energy Neutrinos with MACRO), Proc. of the VIth Neutrino Telescope Workshop, Venice, p.493 (1994).

AN IMPROVED ANALYSIS OF THE UNDERGROUND MUON DECOHERENCE OBSERVED IN MACRO

INFN/AE–97/28
19 Giugno 1997

ABSTRACT

A sample of 350,000 muon pairs observed by MACRO at a depth larger than 3100 hg/cm^2 has been analyzed and the muon lateral distribution has been compared to the predictions of the HEMAS Monte Carlo code. The analysis includes the evaluation of the detector/analysis features affecting the decoherence curve and the measurement of the detector-independent muon lateral distribution at the Gran Sasso depth. The analysis has been performed with improved methods which reduce possible systematic effects. The results and their implications for cosmic ray physics and hadronic interaction models are presented.

INTRODUCTION

The validity of any result on cosmic ray (CR) composition obtained with indirect measurements depends on the reliability range of the Monte Carlo tools used to simulate the primary CR interaction and the shower development in the atmosphere. Moreover, when dealing with direct measurements performed at energies higher than a few tens of TeV, the simulation of the primary CR interaction inside the detector is required to reconstruct the primary CR energy.

The knowledge of the hadronic interaction features is therefore crucial for any experiment studying CR at UHE. The identification of variables sensitive to the details of the hadronic interaction features and the comparison of real data with the Monte Carlo codes play therefore important roles. The MACRO experiment (Ahlen et al., 1993a) performed a detailed study of the cosmic ray composition (Ambrosio et al., 1997) using the HEMAS code (Forti, 1990) to simulate the interaction of primary cosmic rays in the atmosphere. A few years ago, it was pointed out that this code could produce too much P_t (Gaisser, 1993). This hypothesis has been recently restated (Soudan2, 1997). We are going to show in this paper that, despite these theoretical speculations, the HEMAS code properly reproduces the feature of the muon pair separation distribution (decoherence function), a distribution which is very sensitive to the P_t modeling in the Monte Carlo hadronic interaction code (Figure 1). A first attempt to measure the decoherence function with MACRO was performed in MACRO (Ahlen et al., 1992 and 1993b). We present at this conference an improved analysis, in which two different analysis methods were used. The comparison of real data with the Monte Carlo prediction has been performed with special care to avoid possible systematic effects. Moreover, in the present analysis a larger statistical sample is used.

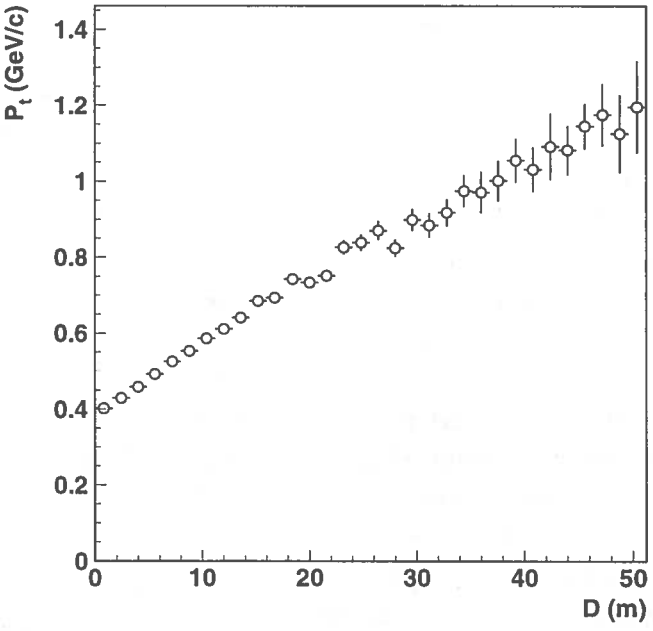

Fig. 1: Average muon parent P_t as a function of the distance between muon pairs at Gran Sasso depth, as computed with the HEMAS code.

DATA ANALYSIS

Apparatus effects cause an unavoidable distortion of the decoherence function. Although MACRO is a large area underground experiment (the largest presently running), the finite size of the detector still has to be accounted for. Although muon pairs with separation D$\simeq$ 70 m can be detected, the apparatus acceptance decreases with the pair distance. Moreover, in a projective apparatus like MACRO the efficiency for unambiguously reconstructing and associating a track in three dimensions has to be evaluated with care. A detailed simulation is therefore required to take into account all these experimental effects. To fulfill the requirements quoted above, we simulated our detector using the GEANT package. Monte Carlo and real data are processed using the same analysis chain. We simulated the interaction of approximately $3.6 \cdot 10^8$ primaries in the atmosphere, using the HEMAS code, according to the MACRO favoured composition model (Ambrosio et al., 1997) inferred by muon multiplicity distribution studies. Folding simulated data with detector simulation is a delicate step. In order to save as much data as possible and to avoid any systematic effects, we used the variance reduction technique (Battistoni et al., 1997), obtaining a sample of $\simeq$1,100,000 simulated muon pairs. Selected runs were used in the real data analysis: we processed about 250,000 muon bundle events ($\simeq$520,000 muon pairs) observed during $\simeq$7000 h of live time. Some cuts have been applied on both the real and the simulated data so that we selected:

- only tracks reconstructed in the wire and strip views, unambiguously associated;
- only "clean" events ($\leq$45 streamer tube fired outside of the tracks);
- only bundles whose average zenith angle is smaller than 60°, to be consistent with the mountain map used in the Monte Carlo;
- only parallel tracks, to reduce the important source of background coming from locally produced hadrons through muon photonuclear processes.

To enforce the cut on the "clean" topologies, we computed the ratio R between the number of streamer tube (ST) wires fired and the number of ST wires expected to be fired, considering the track direction. We accepted only tracks with R$\geq$0.75. Each pair of the bundle has been then weighted with the factor $\frac{2}{n_\mu(n_\mu-1)}$, where n_μ is the number of tracks in the bundle which survived the cuts. After the cuts we have about 350,000 real and 690,000 simulated pairs. We analyzed both the real and the Monte Carlo data with the same software programs (detector dependent curve comparison). Figure 2 shows the comparison between the HEMAS model and the real data. Muon pairs as far as $\simeq$ 70m apart are successfully measured by MACRO; a nice agreement with the Monte Carlo prediction is evident, showing the HEMAS capability in reproducing CR features deep underground. To obtain the muon lateral distribution at the Gran Sasso depths, we evaluated the detection/selection efficiency $\epsilon = \epsilon(D,\theta,\phi)$ by comparing the number of muon pairs in input to the GMACRO simulator and the number of pairs surviving the cuts quoted above, in each bin of (D,θ,ϕ).

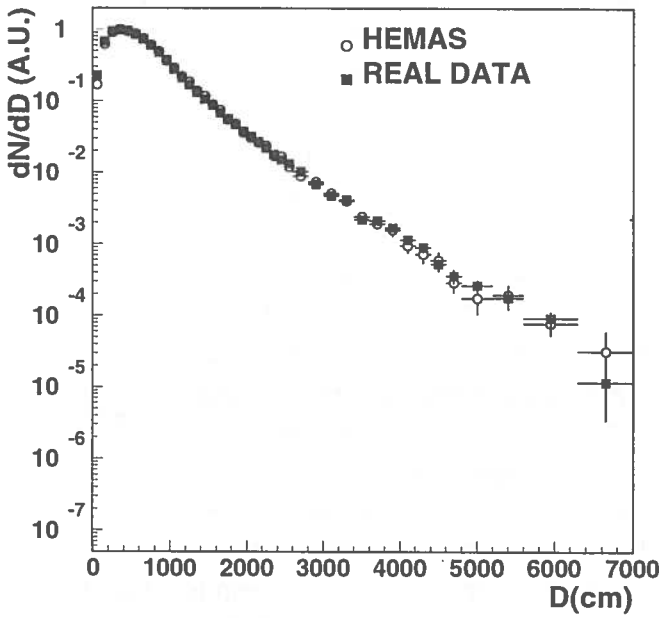

Fig. 2: Decoherence distribution obtained using the detector dependent method (see text), compared to Monte Carlo expectation.

A first attempt to compute $\epsilon(D,\theta,\phi)$ was performed (Ahlen et al., 1992, 1993b) using just muon pairs. This approach overestimated the detection/selection efficiency at small muon separation, because the selection probability of a muon pair is affected by the presence of the other tracks in the bundle ("shadowing effect"). In the present approach, we considered muon bundles generated by HEMAS, following a realistic multiplicity distribution. Then we computed $\epsilon(D,\theta,\phi)$ for each pair. The "shadowing effect", due to multiple tracks, is therefore accounted for. Corrected real data are finally compared directly with the HEMAS simulation. The unfolding procedure requires very high Monte Carlo statistics, so the unfolding is possible only for separation D$\leq$ 50 meters. Figure 3 shows the comparison between Monte Carlo and real data.

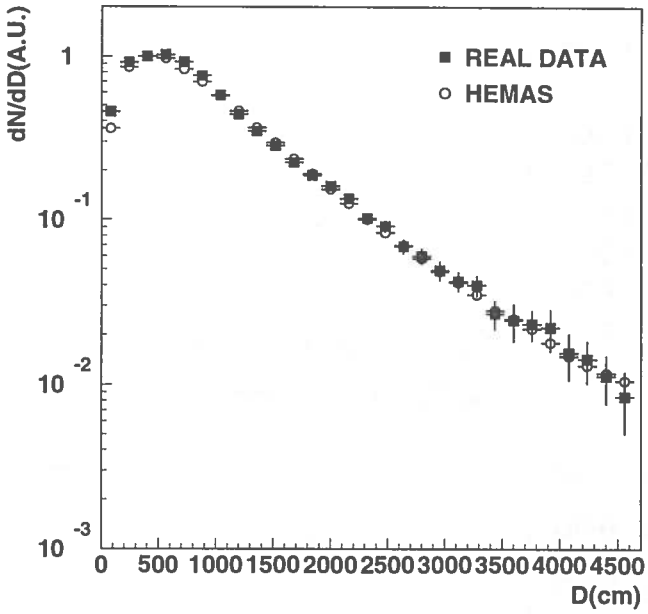

Fig. 3: Decoherence distribution obtained using the detector independent method (see text), compared to Monte Carlo expectation (HEMAS code and MACRO FIT composition model).

A good agreement is evident looking at the plot, confirming the capability of the HEMAS model in reproducing real data features. Further checks on the reliability of the HEMAS hadronic interaction model have been performed, comparing real data and Monte Carlo decoherence in different rock depth and cosθ windows. As an example, we show in Figure 4 the decoherence function in the ranges 0.9$\leq$cosθ $\leq$1.0 and 0.7$\leq$cosθ $\leq$0.8, for 3750 hg/$cm^2\leq$ depth $\leq$ 4150 hg / cm^2. Figure 5 shows the average distance between muon pairs <D>, as a function of cosθ (upper plot) and as a function of the rock depth (lower plot). <D> is found to decrease with cosθ: this is a geometrical effect. Muon pairs originated at larger θ come from primary CR interacting farther from the detector: muons go through larger atmosphere depth before reaching the apparatus. Since muons are divergent, the resulting separation is wider. Deeper depth selection reflects in higher muon energy selection. Since the muon parent meson energy increases roughly linearly with the centre of mass energy $\sqrt{s}$ (while their $<P_t>$ increases with $\sqrt{s}$ only logarithmically), their angular separation, $\psi \simeq P_t/P$, tends to become smaller and therefore the muon separation is less. The agreement between real data and Monte Carlo is satisfactory, confirming the HEMAS capability in reproducing real data in both rock depth and cosθ windows.

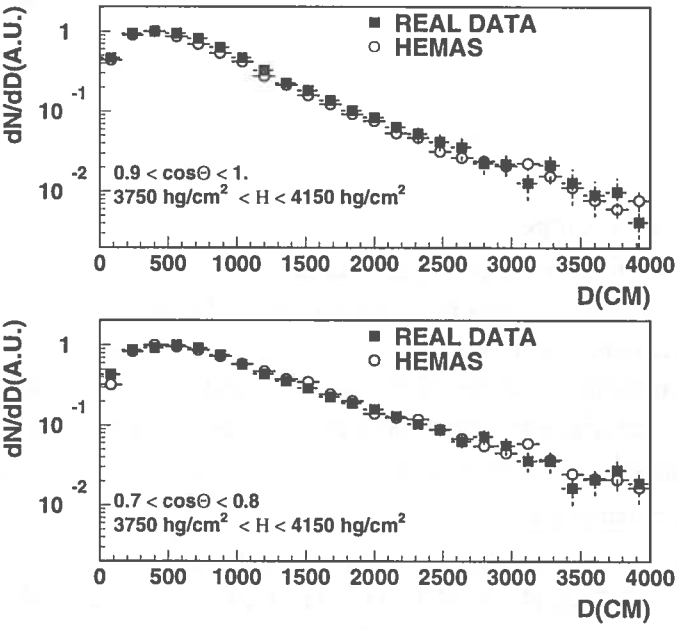

Fig. 4: Detector independent decoherence distribution in the ranges 0.9$\leq cos\theta \leq$1. , 0.7$\leq cos\theta \leq$0.8, for 3750 hg/$cm^2\leq$ depth $\leq$ 4150 hg/cm^2.

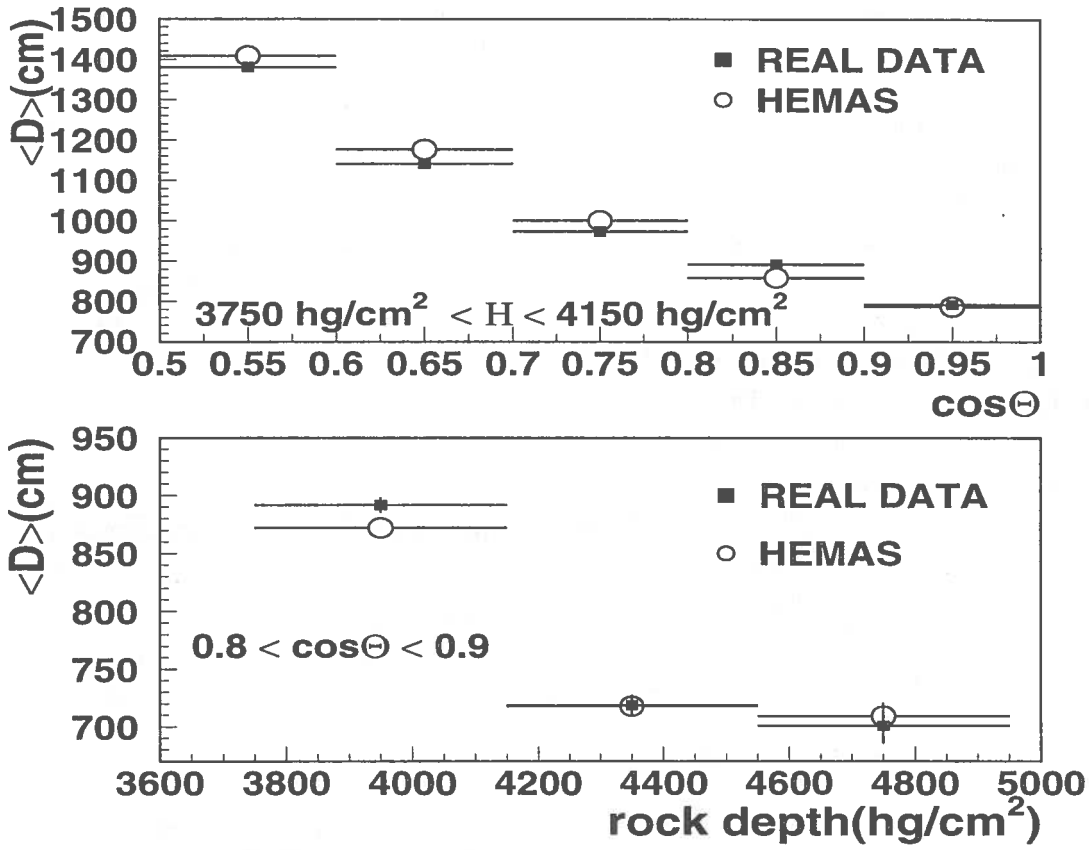

Fig. 5: Average distance between muon pairs <D>, as a function of cosθ and rock depth.

CONCLUSION

We verified that the HEMAS code reproduces the separation distribution of real data. This result has been verified by selecting both cosθ and rock windows. We stress that the study of the decoherence function is an important tool to verify the capability of the Monte Carlo codes in correctly reproducing muon bundle features deep underground. As far as the decoherence is concerned the HEMAS code gives satisfactory results and this makes us confident in using this code for primary CR composition studies.

REFERENCES

Ahlen S. P. et al., MACRO Collaboration, *Nucl. Instr. Meth.* A **324**, 337, (1993a)

Ahlen S. P. et al., MACRO Collaboration, *Proc. 23rd ICRC, Calgary*, **2**, 93 (1993b)

Ambrosio M. et al., MACRO Collaboration, to be published in *Phys. Rev. D (1997)*

Battistoni G. et al., "Monte Carlo simulation of Underground muon events in a finite size detector", to be published in *Astr. Phys.*, (1997)

Forti C. et al, *Phys. Rev. D* **42**, 3668,(1990).

Gaisser T. K., *Proc. Vulcano Workshop 1992 "Frontier Objects in Astrophys. and Particle Phys."*, **40**, 433 (1993)

The SOUDAN2 Collaboration, preprint hep-ex/9612004 v2 (1997) to be published in Phys. Rev. D.

MEASUREMENT OF UNDERGROUND MUON ENERGIES USING A TRD IN MACRO

INFN/AE–97/26
19 Giugno 1997

ABSTRACT

The MACRO detector is located in the Gran Sasso Laboratory. MACRO's overburden varies from 3150–7000 hg/cm^2. A transition radiation detector (TRD) has been added to the MACRO detector in order to measure the energy of muons entering MACRO. At the top of the Gran Sasso, cosmic ray muons must have a threshold energy of 1.4 TeV to reach the MACRO detector. We measure the residual energy of cosmic ray muons, the energy they have after passing through the Gran Sasso and reaching the MACRO detector. Our transition radiation detector consists of three identical modules with a total horizontal area of 36 m^2. The results presented here were obtained with the first module collecting data for almost one year. The average residual energy of downgoing single muons, cut to retain muons below 930 GeV (our TRD saturation energy), is about 200 GeV.

INTRODUCTION

The muon energy spectrum deep underground can be derived from the surface muon spectrum and from calculations of energy losses, using assumptions on the interaction cross sections of high energy muons in the rock. A direct measurement of this spectrum therefore can give information on the interaction mechanisms of muons in the rock, and can be used to confirm the surface muon spectrum and the "all-nucleon" primary cosmic ray spectrum.

In order to increase the MACRO detector capabilities with a device able to measure the residual muon energy we designed and built a large area TRD. The TRD measures the energy of each muon up to the TeV region, although with modest resolution. This measurement may open a wide range of experimental opportunities for cosmic ray physics in underground laboratories. With this technique, the residual energy of downgoing and (neutrino induced) upgoing muons is directly measured.

THE MACRO TRD

Transition radiation (TR) is emitted in the X-ray region whenever an ultrarelativistic charged particle crosses the boundary of two materials with different dielectric properties. For each interface the emission probability for an X-ray photon is of the order of $\alpha = 1/137$ (fine structure constant). Radiators consisting of some hundreds of foils regularly spaced are used to enhance X-ray production; a few photons are produced allowing a reliable tagging of the fast particle. Due to the characteristic dependence (in a limited energy range) of transition radiation on the Lorentz factor γ of the incident particle, it is possible to evaluate its energy $E = m_o\gamma c^2$ in this range if the rest mass m_o is known, or if the particle has been identified, as is the case of muons reaching an underground laboratory. The multilayer radiator introduces physical constraints for the radiation yield, due to the so called "interference effects". The radiation emission practically starts at a Lorentz factor $\gamma_{th} = 2.5\omega_p d_1$, where ω_p is the plasma frequency (in eV units) of the foil material, and d_1 is its thickness in microns. At higher γ the radiation energy increases up to a saturation value $\gamma_{sat} \sim 0.6\gamma_{th}(d_2/d_1)^{1/2}$, where d_2 is the distance of the gap between the foils. Similar behaviours have been observed for irregular radiators such as carbon compound foam layers or fiber mats, where the role of the thin foil is played by the cell wall and by the fiber element, and the gap by the cell pore and by the fiber spacing. A detailed description of TR can be found in (Artru et al., 1975).

The MACRO TRD consists of three modules of 36 m^2 total aerea. Each module has an active volume of $6 \times 1.92 \times 1.7$ m^3 and contains 10 planes of 32 proportional tubes, 6 meters long and with a square cross section of 6×6 cm^2. These counters are laid close together between 11 Ethafoam radiator layers of 10 cm of height to form a large multiple layer TRD with reduced inefficient zones. A detailed description of the MACRO TRD is given in (Barbarito et al., 1995). In Figure 1 we show the TRD response, namely the average number of hits at various γ and various beam crossing angles, as measured in a test beam at CERN P.S.

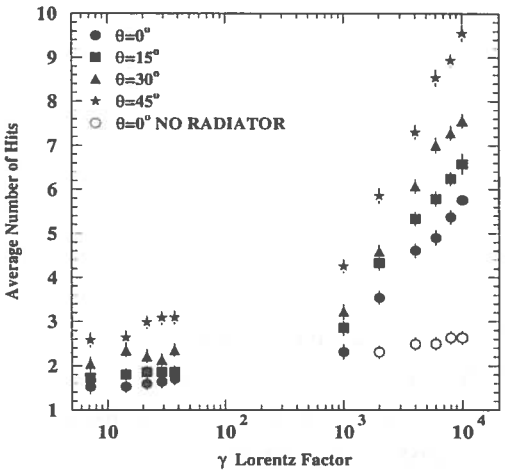

Fig. 1: Average total number of hits for various values of the γ factor : dots: 0° incident beam angle; open circles: 0° beam angle without radiator; squares: 15° beam angle; triangle: 30° beam angle; stars: 45° beam angle.

The MACRO detector is located in Hall B of the Gran Sasso Underground Laboratory. The lab is located at an average depth of 3700 hg/cm^2, with a minimum depth of 3150 hg/cm^2. At these depths the residual energy differential distribution of the downgoing muon is estimated to be nearly flat up to 100 GeV and it falls rapidly in the TeV region; the mean value is a few hundred GeV. The TRD has been designed to explore the muon energy range of 100 GeV–1 TeV. Below 100 GeV there is no TR emission; from 100 GeV to 1 TeV the detector has a smoothly increasing response versus γ. For energies greater than 1 TeV, where the muon flux is estimated to be approximately 5% of the total, the TR signal is saturated.

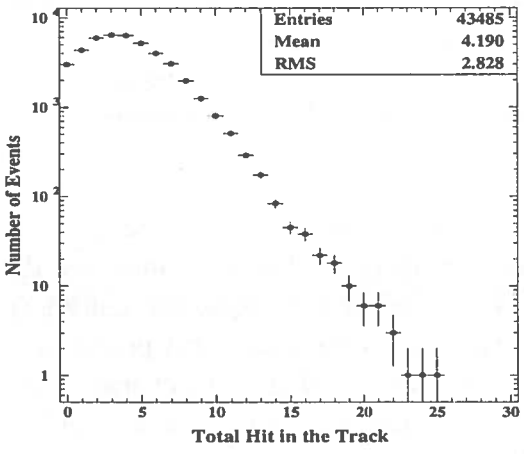

Fig. 2: Hit distribution for single muon tracks crossing the TRD. Only statistical errors are shown.

DATA SELECTION

In this analysis we have considered the data collected from April 1995 to March 1997 by the first TRD module. Since the TRD calibration was performed for particles crossing the ten layers and at zenith angles below 45°, in the analysis only single muons fulfilling these constraints have been included; the analysis method is described in detail in (Ambrosio et al., 1996a). The total number of hits in the track is evaluated by counting the number of TRD hits (in the view perpendicular to the anode wires) along the straight line fitted to the track reconstructed by the MACRO detector. In Figure 2 we report the distribution of the number of hits in the track for these muons.

MUON ENERGY SPECTRUM

In order to evaluate the local muon energy spectrum, we must take into account the TRD response function, which induces some distortions of the "true" muon spectrum distribution. The "true" distribution can be extracted from the measured one by an unfolding procedure that yields good results only if the response of the detector is correctly understood.

We have adopted an unfolding technique, developed according to Bayes' theorem, following the prescriptions of (D'Agostini, 1995) and (Mazziotta, 1995). Usually the unfolding methods require that the independent variable (the energy) is limited inside a finite interval. When it is practically

boundless, as for the cosmic ray energy spectrum, the method cannot be automatically applied. However, in our case this problem can be overcome since the detector response is flat outside the 100 GeV–1 TeV energy interval; thus the number of hits related to the energy is effectively "bounded".

Detector simulation

The distributions of the hits collected along a muon track by the TRD at a given zenith and azimuthal angle, $N(k, \vartheta, \varphi)$, can be related to the residual energy distribution of muons, $N(E, \vartheta, \varphi)$, by:

$$N(k, \vartheta, \varphi) = \sum_{j=1}^{n_E} p(k \mid E_j, \vartheta, \varphi) N(E_j, \vartheta, \varphi) \qquad (1)$$

where the detector response function, $p(k \mid E_j, \vartheta, \varphi)$, represents the probability to observe k hits for a track of a given energy E_j and at a given angle ϑ and φ. The response function must contain both the detector acceptance and the event reconstruction efficiency. We have derived the response function simulating the MACRO behaviour using GEANT (Brun et al., 1992), including the trigger efficiency simulation. The simulation of the TRD was based on the test beam calibration data (Figure 1), taking also into account the inefficiency of the proportional tubes. A check of the response function of the TRD is obtained using low energy muons, namely stopping muons and muons with large scattering angle in MACRO, which have energies of about of 1–2 GeV.

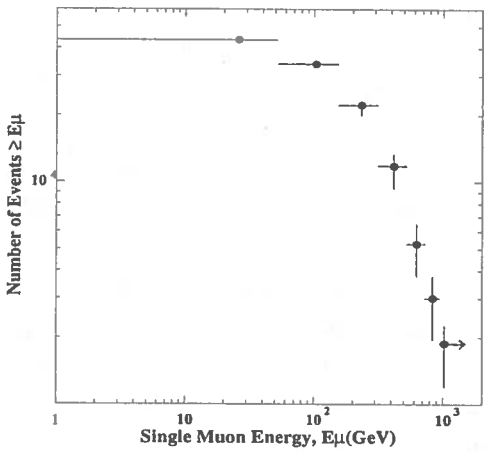

Fig. 3: Integral energy distribution of single muons in the TRD. The last bin to the right is relative to energies larger than saturation (930 GeV). Horizontal bars are the bin width, while vertical bars are the total error (statistical and systematic).

Experimental data distributions

The unfolding procedure described above was applied to the TRD experimental data, starting with a trial spectrum assigned to the unfolded distribution (D' Agostini, 1995; Mazziotta, 1995), according to a local energy spectrum of muons at 4000 hg/cm^2 with a spectral index fixed at 3.7 given by (Lipari and Stanev, 1991):

$$N_o(E, \vartheta, \varphi) \sim e^{-\beta h(\alpha-1)} (E + \epsilon(1 - e^{-\beta h}))^{-\alpha} \qquad (2)$$

The parameters are: $h = 4\ km\ w.\ e.$, $\alpha = 3.7$, $\beta = 0.383\ (km\ w.\ e.)^{-1}$ and $\epsilon = 0.618\ TeV$.

Because the TRD behaviour shows a saturated region (for $E_\mu \geq 930$ GeV), then in that range only the number of events can be evaluated, while below 930 GeV we can reconstruct the energy distribution and we can compute the average value cut to 930 GeV. Figure 3 shows the muon integral spectrum. Figure 4 shows the average muon energy cut to 930 GeV, as a function of the rock depth. The error bars include statistical and systematic uncertainties. The systematic errors have been evaluated by the search of low energy events in the TRD.

DISCUSSION AND CONCLUSION

The muon spectrum deep undergound is determined by the spectrum at the surface and the energy losses in the rock. The muon spectrum at surface is sensitive to the "all-nucleon" spectrum of primary cosmic rays. We have compared our results to the predictions from two extreme hypotheses on the primary spectra (Ambrosio et al., 1996b), namely the "Light" (Fitchel and Linsley, 1986) and the "Heavy" (Goodman, 1982) compositions. However, the mean primary energy that gives a single muon underground is rather similar in the two models (Forti et al., 1990). So the average muon energy underground for single muons is still equivalent for both models.

The interaction of the cosmic rays in the atmosphere was simulated with the HEMAS code (Forti et al., 1990). The produced muons at the surface were then propagated through the rock, with the muon energy loss in the rock evaluated according to the prescriptions of (Lipari and Stanev, 1991). The rock thickness was calculated at each ϑ and φ from the Gran Sasso map (MACRO, 1995). We used the correction procedure described in (Wright et al, 1973) for the conversion to standard rock.

Figure 4 shows the average single muon energies relative to the two predictions taking into account the saturated region of the TRD, together with experimental data (lower part of the figure). Due to the saturation of the TRD, the average energy computed in this way underestimates the real measurement, as is shown in the upper part of the same figure. The average muon energies (cut to retain energies below 930 GeV) for the above models have been evaluated using 6 bins as for the real data; while for the uncut case no binning procedure has been used.

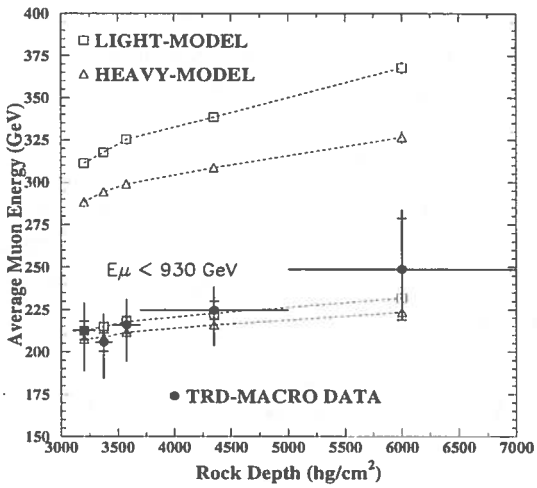

Fig. 4: The lower part of the picture shows the average single muon energy, cut to 930 GeV, versus the standard rock depth. The experimental data are shown together with the predictions of two primary composition models. In the upper part of the figure, the same distributions, with the same symbols, for the uncut case are shown. The extentions of the statistical error bars represent the estimates of systematic uncertainties. The dotted lines are drawn to guide the eye.

We have measured directly the residual energy of cosmic ray muons crossing the MACRO detector at the Gran Sasso underground laboratory, using a TRD which took data since April 1994. The average single muon energy, removing energies above 930 GeV, is found to be $216 \pm 5 \pm 18$ GeV in the depth range 3150–7000 hg/cm^2. In this way we can estimate that the average single muon energy is about 300–330 GeV at the MACRO depth.

Our experimental data, after corrections for the propagation of the muons through the Gran Sasso rock, are consistent, within the errors, with the above predictions. The present precisions do not allow us to distinguish between the above models.

REFERENCES

Ambrosio, M. et al.,MACRO Collaboration, Phys. Rev. D **52** (1995) 3793.
Ambrosio, M. et al.,MACRO Collaboration, MACRO/PUB 96/6 (1996).
Ambrosio, M. et al.,MACRO Collaboration, INFN/AE-96/29 (1996).
Artru, X., Yodh, G. B. and Mennessier, G., Phys. Rev. D **12** (1975) 1289.
Barbarito, E., Bellotti, R., Cafagna, F. et al., Nucl. Instr. and Meth. A **365** (1995) 214.
Brun, R. et al., CERN Public. DD/EE/84-1 (1992).
D'Agostini, G., Nucl. Instr. and Meth., A **362** (1995) 487.
Ficthel, C. and Linsley, J., Astrophys. J. **300** (1986) 474.
Forti, C., Bilokon, H., d'Ettore Piazzoli, B. et al., Phys. Rev. D **42** (1990) 3668.
Goodman, J. A., Ellsworth, R. W., Ito, A. S. et al., Phys. Rev. D **26** (1982) 1043.
Lipari, P. and Stanev, T., Phys. Rev. D **44** (1991), 3543.
Mazziotta, M. N., LNGS 95/52, (1995).
Wright, A. G., Proc. of 12th ICRC, Denver (USA), **3** (1973) 1709.

A SKY SURVEY USING MUONS IN THE MACRO DETECTOR

INFN/AE–97/27
19 Giugno 1997

ABSTRACT

During 1991 - 1996 we have detected more than 2×10^7 muons in MACRO, which is located at the Gran Sasso Laboratory. Our effective livetime is 26,400 h. Using this sample of data we have defined and evaluated MACRO's properties as a muon telescope. First we observed the Moon shadowing effect. This is the first statistically significant detection of the moon using muons detected deep underground. Our detection of this signal has established that the pointing errors of MACRO are less than 0.1 degree and that the angular resolution of the apparatus is about 1 degree. Next we studied the arrival directions of muons, looking for excesses above the expected background in any direction of the sky. Finally we have also done a detailed search for possible muon point sources (and diffuse sources) in the galactic plane using double muons. We will present all three results; the Moon shadowing, the sky survey, and the flux limits for muon sources in the galactic plane.

INTRODUCTION

In this work we have used the directionality of the muons seen by the MACRO detector to survey the sky for steady sources of muon excesses. The analysis has been done using the muons collected during 1991-1996. We have thus collected more than 2×10^7 muons. The interest for this analysis arises from the old observations of excesses of underground muons in the direction of Cygnus X-3. More recently no signal has been detected from this kind of source but several observations of X or γ ray bursts have been reported from other sources like Mkn 421 (Bradbury et al. 1997). Therefore the interest for a monitoring of any possible source of cosmic rays is still present. However the underground detectors can detect only the secondary muons produced in the interactions of the primary cosmic rays with the atmosphere. So their sensitivity to cosmic ray sources is lower than that of surface and satellite experiments. Nevertheless MACRO can detect very small variations of underground muon intensity. In fact we have reported the measurement of a seasonal variation of the intensity (Ambrosio et al., 1997), in which a modulation of the intensity with an amplitude of less than 3% is found. We have also observed the moon shadowing effect on the intensity (Ambrosio et al., 1997). This last effect is extremely important in establishing the correctness of the pointing ability and at the same time the good angular resolution of the apparatus.

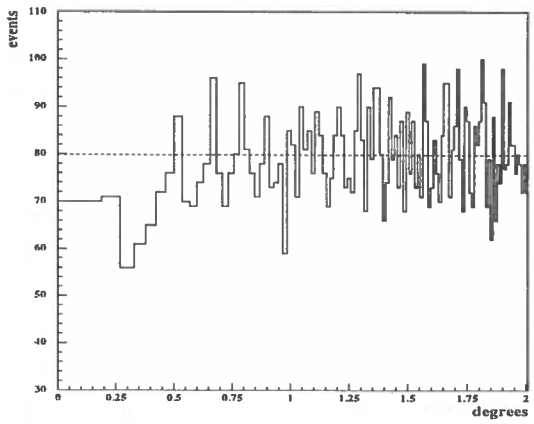

Fig. 1: Muon density versus the angular distance from the Moon. Superimposed as a dashed line is the expected density for the background events. A variable bin width is used in order to have the same solid angle for each bin.

THE MOON SHADOWING EFFECT

To verify the pointing accuracy of the MACRO detector, we have searched for the Moon shadowing effect in the high energy primary cosmic rays. This analysis has been done using all muons collected by the detector from 1989 to the beginning of 1997. The resulting sample is about 30×10^6 muons. The analysis has been done selecting single or multiple muons having the arrival directions close to the moon center, and comparing the distribution of these events with the dis-

tributions of random background events. The analysis has been done using two different methods: the first one is a simple comparison of the density of the real and simulated event distributions versus the angular distance from the Moon center. The results are shown in Figure 1. A deficit is visible at about 0.25 ° from the computed Moon position and the maximum resulting deficit is about 130 events on a background of 2218 ±47 events contained in a cone of about 1° radius centered on the Moon position.

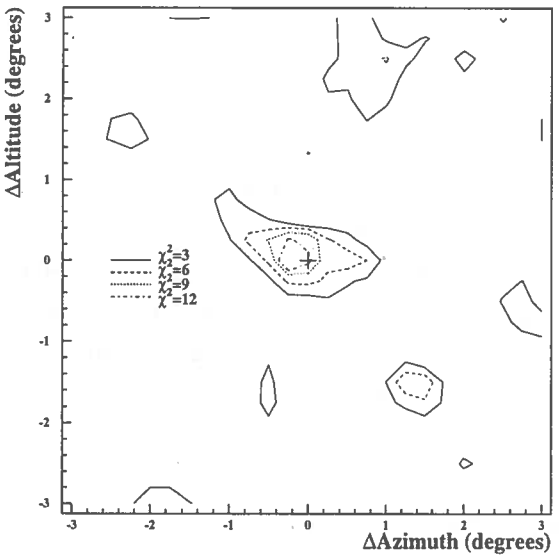

Fig. 2: χ^2 levels in the window centered on the Moon. Four levels starting from χ^2=3 with a step of 3 are shown. The maximum value is χ^2=14.2 in the position (-0.25°,0°)

A second analysis has been done using bidimensional histograms and taking into account the point spread function of the apparatus. This analysis is based on the maximum-likelihood method of COS-B (Pollock et al., 1993) to evaluate the significance of the signal (Ambrosio et al., 1997). The results of this analysis are shown in Figure 2, where the χ^2 in each bin has been computed as a function of the Altitude versus Azimuth distances from the Moon center. The amount of the displacement found can be attributed to the geomagnetic displacement of the primary protons, which have energies of about 10 TeV. We found therefore a westward displacement of 0.25° of the Moon shadow with a χ^2=14.2 corresponding to a significance of 3.7σ. We have compared this number with an analysis done on random fake moons. We found that the probability to find random fluctuations having a $\chi^2 \geq 14.2$ is 0.02%, in agreement with the previous estimation of the significance. Thus this positive identification of the moon shadowing effect in an undergound experiment establishes the correct pointing ability of the detector.

ALL-SKY SURVEY USING SINGLE MUONS

We have grouped the events in sky bins of equal solid angle ($\Delta\Omega = 2.3\times10^{-4}$, $\Delta\alpha = 1°$, $\Delta sin\delta = 1/75$). These bins have approximately the solid angle of a cone of half-angle 1.°, a value obtained to maximize the signal to noise ratio for our apparatus. Removing from the sample the bins having few events, we compute for each bin the standard deviation using the simple Gaussian statistics $(n_{obs} - n_{bck})/\sqrt{n_{bck}}$, where n_{obs} and n_{bck} are the observed and expected events respectively. This distribution is well fitted by a Gaussian curve and no excess is evident. The result of the fit gives χ^2/Dof=0.86. We have repeated the survey by displacing the center of these bins, in both the coordinates, of half of the bin width, in order to search for possible sources close to the neighborhoods of the bins. No excess has been found also in this case. We thus confidently say that no significant "point source" has been observed.

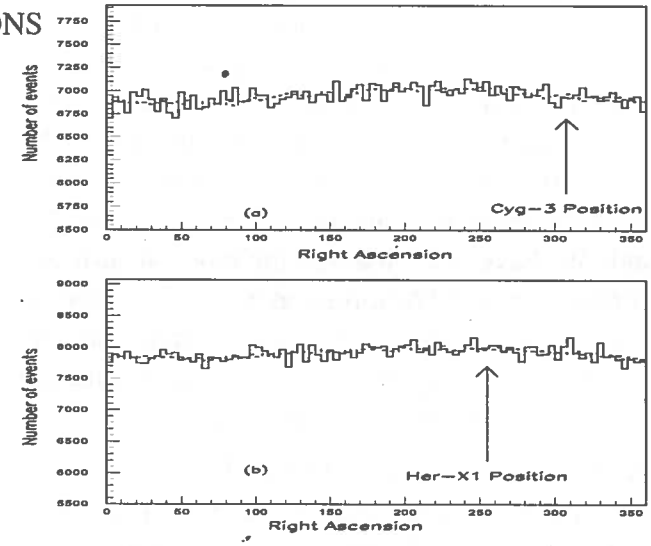

Fig. 3: Right ascension distributions for muons coming from a 1.5° half angle declination window centered on (a) Cyg X-3 and (b) Her X-1. Solid lines represent the experimental data and dashed the background simulation.

against the seasonal modulation, the fit to the antisidereal diurnal data gives the parameters in the relation: $K_2 \cos\{2\pi[(N_{sol}-1)t+\phi_1-\phi_2]\}$. In this fit, ϕ_{max} in Table 1 was shifted to account for the arbitrary zero point of phase used in constructing Figure 2. As shown in Ambrosio et al. (1997), the phase of maximum modulation for the seasonal variation is $\phi_2 \approx 0.6$, which implies that $\phi_{max} \approx 0.45$ for the antisidereal modulation. Finally, the sidereal modulation seen in Figure 3, parameterized as $K_3 \cos\{2\pi[(N_{sol}+1)t+\phi_3]\}$, is the 'apparent sidereal modulation' and represents the sum of two terms,

$$K_3 \cos\{2\pi[(N_{sol}+1)t+\phi_3]\} = K_4 \cos\{2\pi[(N_{sol}+1)t+\phi_4]\} + K_2 \cos\{2\pi[(N_{sol}+1)t+\phi_1+\phi_2]\}.$$

The amplitude, K_4, and the phase, ϕ_4, of the 'true sidereal modulation' can be found from the fits in Table 1. The results of this analysis, including the correction for the zero point of antisidereal phase and the converstion from Julian days to solar time, are given in Table 2. The errors on K_4 and ϕ_4 were computed by combining the errors in quadrature.

Table 2: Analysis of Underground Muon Data

	Amplitude (%)		Phase of Maximum (hr)	
Solar Diurnal	0.093 ± 0.063	(K_1)	13.2 ± 2.6	(ϕ_1)
Antisidereal	0.17 ± 0.05	(K_2)	10.8 ± 1.4	$(\phi_1 - \phi_2)$
Apparent Sidereal	0.19 ± 0.06	(K_3)	5.9 ± 1.3	(ϕ_3)
True Sidereal	$0.34 \pm .26$	(K_4)	4.8 ± 3.2	(ϕ_4)

CONCLUSIONS

We have used the method of Farley and Storey (1954) to search for the first harmonic of the sidereal modulation in the underground muon data collected by MACRO. The result at this time must be considered preliminary. In order to achieve a result with high statistical significance, several more years of MACRO data must be analyzed.

REFERENCES

Alexeenko, V.V., et al. Proc. 23rd ICRC, 1, 483 (1993).
Ambrosio, M., the MACRO Collaboration, Astroparticle Phys., in press (1997).
Borione, A., et al., Astrophys.J., preprint (1996).
Compton, A.H., and Getting, I.A., Phys.Rev., 47, 817 (1935).
Farley, F.J.M., and Storey, J.R., Proc.Phys.Soc., 67, 996 (1954)
Hall, D.L., Duldig, M.L., and Humble, J.E., Space Sci.Rev., 78, 401 (1996).
Nagashima, K., et al., il Nuovo Cimento, 12, 695 (1989).

POINT SOURCE STUDIES

Steady Flux Limits

As a first step, we selected only muons coming from two windows $\pm 1.°$ wide in declination centered on Cyg X-3 and Her X-1 and we searched for dc excesses in the muon flux above the expected background in the Right Ascension distributions around those positions. No excess was found around the two source positions.

We also searched the data for other particular point sources (see Table 1). We analyzed the data contained in a narrow cone (0.5° radius) around the source position and found no dc excess. The dc upper flux limits, using the formula (Ahlen et al., 1993):

$$J_{\mu}^{stdy} = \frac{n_{\mu}(95\%)}{0.41 \epsilon A_{eff} f t_{expos}} cm^{-2} s^{-1} \qquad (1)$$

are presented in Table 1, with $n_{\mu}(95\%)$ the 95% CL for the undetected number of muons calculated according to Helene (Helene, 1983), ϵ the average efficiency, A_{eff} the average effective area, f is the fraction of time that the source is visible, and t_{expos} the total exposure time.

Source	δ	f	$(\epsilon \cdot A_{eff}) \times 10^4 cm^2$	$J_{\mu}^{stdy}(95\%)$ $(cm^{-2}s^{-1})$
Cyg X-3	40°55′46”	0.57	724	3.9×10^{-13}
Her X-1	35°20′32”	0.52	738	4.7×10^{-13}
Crab	21°59′	0.48	758	5.5×10^{-13}
3C273	2°3′8”	0.37	618	7.0×10^{-13}
MRK 421	38°12′31”	0.58	730	4.5×10^{-13}
Geminga	17°47′	0.46	743	5.1×10^{-13}

Table 1: *Steady Flux Limits for selected sources. Limits were obtained using formula (1).*

Since there is no excess in all other bins in the sky, we have also calculated the flux limits using (1). The results of this all-sky map give flux limits in the interval $8.2 \times 10^{-14} cm^{-2}s^{-1} \rightarrow 8.5 \times 10^{-13} cm^{-2}s^{-1}$.

Searches for Modulated Signals

A careful search has been done for modulated signals coming from those sources that in the past showed variability (Cyg X-3). We found no evidence for an excess in any of the phase bins into which the characteristic period was divided. The flux limit for modulated signals at 95% C.L. found for Cyg X-3 is $9.7 \times 10^{-14} cm^{-2}s^{-1}$.

We conclude that the present data are consistent with background fluctuations and show no evidence for a modulated muon signal from Cyg X-3.

A Galactic Plane Survey Using Double Muons

A different point source investigation has been performed selecting only double muons in the apparatus. There are two reasons to select these events in underground detectors. The primary cosmic ray average energy necessary to produce underground muons is higher for multiple muons respect to single muons. In addtion, it has been suggested (Stanev 1986, Berezinsky 1988 and Halzen 1997) that primary gamma rays would produce double muons through photoproduction processes. However the limits of this kind of search are related to the efficiency to have muons starting from γ rays. In fact the probability to produce muons by means of γ rays is about 1% at TeV energies. For this analysis therefore we have used the subsample of events taken between 1991 and 1996 and analyzed the region of the galactic plane delimited by $20° \leq l^{II} \leq 220°$ and $-5° \leq b^{II} \leq 5°$. The analysis has been performed using the same COS-B technique used for the Moon shadowing effect, but using the point spread function in galactic coordinates. The results of this survey are shown in Figure 4.

CONCLUSIONS

A search for cosmic ray point sources has been performed using underground muons and different analyses. No evidence for point sources has been found. Nevertheless the MACRO detector has shown its ability to detect a small variation of the muon fluxes, having detected the moon shadowing effect with 3.7 σ significance and the seasonal variation effect.

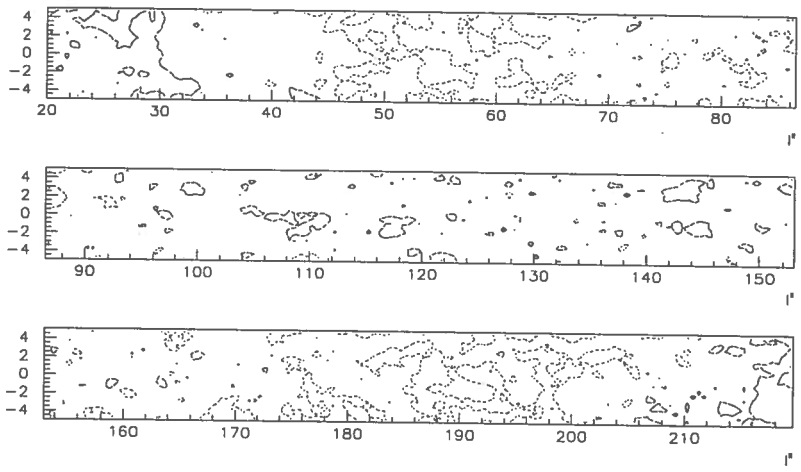

Fig. 4: Distribution of the upper limits for $\Phi_{2\mu}$ in galactic coordinates. The contour levels are from 2.0 to 8.0 $\times 10^{-14} cm^{-2} s^{-1}$.

REFERENCES

Ahlen, S. P. et al., MACRO Collaboration, AJ, **412**, 301 (1993).
Ambrosio, M. et al., MACRO Collaboration, INFN/AE-97/03 (1997).
Ambrosio, M. et al., MACRO Collaboration, accepted by Astrop. Phys. also INFN/AE-97/05 (1997).
Berezinsky, V.S. et al., A&A **189**, 306 (1988).
Bradbury, S.M., et al. (HEGRA Collaboration), A&A, **320**, L5-L8 (1997)
Halzen, F., Stanev, T. and Yodh , G.B., Phys. Rev. D, **55**, 4475 (1997)
Helene, O., Nucl. Inst. Meth. **212**, 319 (1983).
Pollock, A.M.T., et al., A&A, **94**, 16 (1993).
Stanev, T., Phys. Rev. D, **33**, 2740 (1986)

THE SEARCH FOR A SIDERAL ANISOTROPY IN THE UNDERGROUND MUON INTENSITY AS SEEN BY MACRO

INFN/AE–97/28
19 Giugno 1997

ABSTRACT

We have analyzed 39.2×10^6 muons collected in 5.2×10^4 hours of live time by the MACRO detector during the period from 1989 to 1996. Using a high quality subsample of these data, comprising 4.4×10^6 muons, we have searched for modulations consistent with the first harmonic of the solar diurnal, antisidereal, and sidereal periods. The method of Farley and Storey (1954) has been used to obtain the 'true sidereal' modulation. Preliminary results are presented.

INTRODUCTION

During the past 60 years, many searches have been made for a sidereal anisotropy in the arrival directions of cosmic rays. Compton and Getting (1935) initially looked for the sidereal signal arising from the Galaxy's rotational motion through a sea of extragalactic cosmic rays. They argued that a sidereal signal toward the apex of Galactic rotation would provide evidence for an extragalactic component of cosmic rays. Air shower array experiments, which typically are sensitive to cosmic rays with energies in excess of 50 TeV, have continued this search to the present with conflicting results (Kifune, et al. 1986; Nagashima, et al. 1989; Alexeenko, et al. 1993; Borione, et al. 1996). However, shallow underground muon telescopes and neutron monitors, which probe low energy cosmic rays ($E < 100$ GeV), have clearly observed statistically significant modulations with periods of a solar day and a sidereal day in their cosmic ray data (Hall, Duldig, and Humble 1996). These variations are well explained by the effects of the solar wind and interplanetary magnetic fields on lower energy cosmic rays.

MACRO is a large, deep underground detector that is well suited to search for a sidereal modulation of primary cosmic rays. Our sensitivity to weak periodic signals has already been demonstrated by the detection of seasonal variations in the underground muon rate (Ambrosio et al. 1997). MACRO's sensitivity to primary cosmic rays > 5 TeV suggests that the muon data are unlikely to be strongly affected by local interplanetary conditions.

DATA ANALYSIS

The effects we are searching for are smaller than the few percent seasonal variations already reported by the MACRO collaboration. It is therefore essential to define a very high quality data set that is as free of systematic effects as possible. The analysis procedure is based on the method of Farley and Storey (1954) that searches for the first harmonic of the sidereal modulation.

Data Sample

Data were collected during the period beginning in February 1989 and ending in December 1996. During this period, approximately 39.2×10^6 muons were recorded in approximately 5.2×10^4 hours of live time.

We first applied run cuts that ensured that the detector was operating efficiently. Run cuts include: all 6 supermodules in acquisition; streamer tube system operating efficiently; run rates within 3σ of the mean. Within a run individual events were required to cross all 10 horizontal streamer tube tracking planes. Such events have essentially almost 100% probability of resulting in a reconstructed track. These cuts therefore define a data set that requires no corrections for efficiency and they are the same cuts as those used in the search for seasonal variations (Ambrosio et al. 1997). This high quality data sample includes 13.2×10^6 muons.

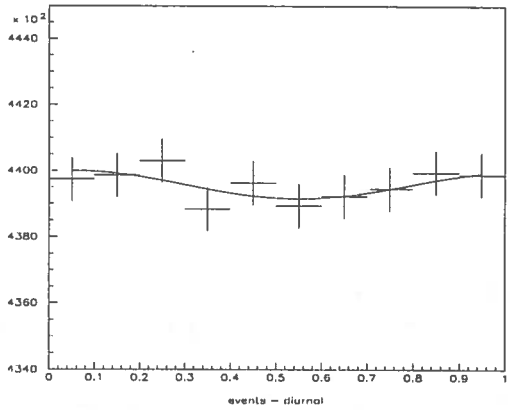

Fig. 1: Solar diurnal variations with fit superposed.

The search for the true sidereal modulation requires a correction for solar diurnal variations. However, solar diurnal variations can be masked by human activities on the detector like detector maintenance and repair, installation, calibration, etc., which typically takes place during the day. At night the detector is usually unattended. Additional cuts were developed to minimize this effect: (1) Gaps between runs were required to be ≤ 3.5 minutes. New runs begin automatically when the data buffers fill, and this proceedure usually takes less than 3.5 minutes. A longer gap between runs ordinarily indicates that a run was terminated manually. (2) Sets of runs with gaps < 3.5 minutes were required to be at least one whole day in length and muons were kept for further analysis only if their arrival times were within an integral number of whole days from the arrival time of the first event of that run set. Studies indicate that including runs with gaps longer than 3.5 minutes introduces significant solar diurnal variations. These cuts reduced the data sample to 4.4×10^6 muons.

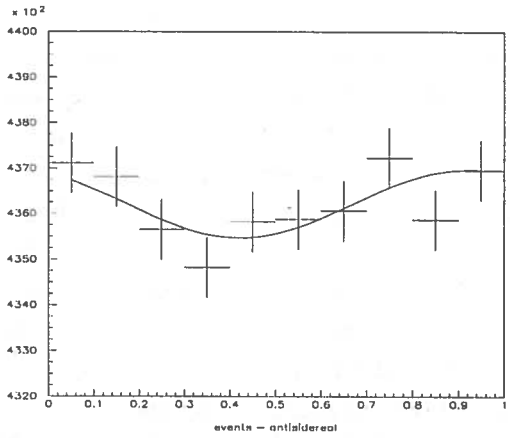

Fig. 2: Antisidereal variations.

Analysis Procedure

Our 'harmonic analysis' procedure (Farley and Storey 1954) first searches for variations in muon arrival times modulated by the solar diurnal period, the sidereal diurnal period, and the antisidereal diurnal period. The length of a solar diurnal period is the mean solar day, t_{sol}; the length of a sidereal diurnal period is the sidereal day, t_{sid}. Let T_{trop} be the length of a tropical

year. Then there are $N_{sol} = T_{trop}/t_{sol}$ solar days in a tropical year and $N_{sol} + 1$ sidereal days in a tropical year. The antisidereal diurnal period is then given by $t_{anti} = T_{trop}/(N_{sol} - 1)$. The data are modulated with the antisideral period because the solar diurnal period beats with the seasonal period, T_{trop}, and a 'sideband' with the period t_{anti} appears. This same beating effect also introduces a 'sideband' with the sidereal period, t_{sid}. It is this faux sidereal modulation that must be removed from the data to find the true sidereal effect (Farley and Storey 1954).

Three phase diagrams were constructed using the data set described above. These phase diagrams differed only in the length of the day used. For the solar diurnal modulation, the Julian day fraction of its arrival time was used to bin each muon; this implies that the zero point of phase is 12^h UT. For the apparent sidereal modulation, the right ascension of its arrival direction was used to bin each muon. The zero point of phase for the antisidereal modulation was arbitrarily chosen as the arrival time of the first muon in the data set. These three (zero-suppressed) phase diagrams are shown in Figures 1, 2 and 3. The error bars are statistical. Since only whole days of data are used, no corrections were necessary for changes in the detector configuration.

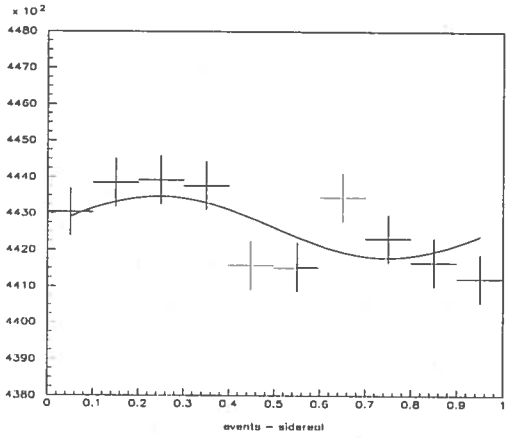

Fig. 3: Apparent sidereal variations.

We searched for the first harmonic of the modulation in the three phase diagrams by fitting the binned muon data to the form:

$$N = < N > + A \cos[2\pi(\phi + \phi_{max})], \tag{1}$$

where $< N >$ is the mean per bin, A is the amplitude of the modulation, ϕ is the phase, and ϕ_{max} is the phase of maximum. The fit parameters are given in Table 1. The curves representing these fits have been superposed on the binned muon data in Figures 1, 2, and 3.

Table 1: Results of Fitting Binned Muon Data

	$< N >$	A	ϕ_{max}	χ^2/dof
Solar Diurnal	4.40×10^5	430 ± 290	$0.05 \pm .11$	0.345
Antisidereal	4.36×10^5	750 ± 280	$0.08 \pm .06$	0.841
Apparent Sidereal	4.43×10^5	840 ± 280	$0.25 \pm .06$	2.26

RESULTS

Vector methods can now be used to extract the first harmonic of the 'true sidereal modulation.' The fit to the solar diurnal data in Table 1 directly yields the fit parameters in the relation: $K_1 \cos[2\pi(N_{sol}t + \phi_1)]$, where K_1 is the solar diurnal amplitude and t is the arrival time of the muon. Since the antisidereal modulation results from the solar diurnal modulation beating

against the seasonal modulation, the fit to the antisidereal diurnal data gives the parameters in the relation: $K_2 \cos\{2\pi[(N_{sol}-1)t+\phi_1-\phi_2]\}$. In this fit, ϕ_{max} in Table 1 was shifted to account for the arbitrary zero point of phase used in constructing Figure 2. As shown in Ambrosio et al. (1997), the phase of maximum modulation for the seasonal variation is $\phi_2 \approx 0.6$, which implies that $\phi_{max} \approx 0.45$ for the antisidereal modulation. Finally, the sidereal modulation seen in Figure 3, parameterized as $K_3 \cos\{2\pi[(N_{sol}+1)t+\phi_3]\}$, is the 'apparent sidereal modulation' and represents the sum of two terms,

$$\begin{aligned} K_3 \cos\{2\pi[(N_{sol}+1)t+\phi_3]\} &= K_4 \cos\{2\pi[(N_{sol}+1)t+\phi_4]\} + \\ & \quad K_2 \cos\{2\pi[(N_{sol}+1)t+\phi_1+\phi_2]\}. \end{aligned}$$

The amplitude, K_4, and the phase, ϕ_4, of the 'true sidereal modulation' can be found from the fits in Table 1. The results of this analysis, including the correction for the zero point of antisidereal phase and the converstion from Julian days to solar time, are given in Table 2. The errors on K_4 and ϕ_4 were computed by combining the errors in quadrature.

Table 2: Analysis of Underground Muon Data

	Amplitude (%)		Phase of Maximum (hr)	
Solar Diurnal	0.093 ± 0.063	(K_1)	13.2 ± 2.6	(ϕ_1)
Antisidereal	0.17 ± 0.05	(K_2)	10.8 ± 1.4	$(\phi_1 - \phi_2)$
Apparent Sidereal	0.19 ± 0.06	(K_3)	5.9 ± 1.3	(ϕ_3)
True Sidereal	$0.34 \pm .26$	(K_4)	4.8 ± 3.2	(ϕ_4)

CONCLUSIONS

We have used the method of Farley and Storey (1954) to search for the first harmonic of the sidereal modulation in the underground muon data collected by MACRO. The result at this time must be considered preliminary. In order to achieve a result with high statistical significance, several more years of MACRO data must be analyzed.

REFERENCES

Alexeenko, V.V., et al. Proc. 23rd ICRC, 1, 483 (1993).
Ambrosio, M., the MACRO Collaboration, Astroparticle Phys., in press (1997).
Borione, A., et al., Astrophys.J., preprint (1996).
Compton, A.H., and Getting, I.A., Phys.Rev., 47, 817 (1935).
Farley, F.J.M., and Storey, J.R., Proc.Phys.Soc., 67, 996 (1954)
Hall, D.L., Duldig, M.L., and Humble, J.E., Space Sci.Rev., 78, 401 (1996).
Nagashima, K., et al., il Nuovo Cimento, 12, 695 (1989).